Chapter 5

Case Studies on Sustainable Use of Ground Source Heat Pumps

This chapter should be cited as

Sakaguchi K. and V. Anbumozhi (2015), 'Case Studies on Sustainable Use of Ground Soruce Heat Pumps', in *Sustainability Assessment of Utilising Conventional and New Type Geothermal Resources in East Asia*. ERIA Research Project Report 2014-41, Jakarta: ERIA, pp.103-155. Available at: http://www.eria.org/RPR_FY2014_No.41_Chapter_5.pdf

Chapter 5

Case Studies on Ground Source Heat Pumps

5.1. China: Investigation, Evaluation, and Monitoring

5.1.1. Introduction: Exponent increase of ground source heat pumps in China

Figure 5.1-1 shows growth of geothermal utilisation in the past 20 years in China. There are different speeds for three types of geothermal use. Geothermal power generation has very little growth only. Geothermal direct use has gentle growth. However, ground source heat pump (GSHP) has an exponential increase.

Figure 5.1-1. Growth of Geothermal Utilisation in China

Source: Edited by authors based on statistics data of the Geothermal Council of China Energy Society.

GSHP has sprung up in China in the past 20 years. Even though the Chinese had studied heat pumps since 1960s, it was only in research by scholars in Tianjin University and Tsinghua University. Tests were carried out in the laboratory and at a few engineering sites. There was no condition for practical application due to the lack of electricity, even for public lighting at that time.

The first GSHP application project was the New Henderson Building in Beijing in 1995. It used the heat pump of the Carrier brand made in the United States. Ten groundwater wells were drilled for pumping-up and reinjection. Since project implementation, Tsinghua University, combining with Shandong Fuerda Co. Ltd., started to develop domestic heat pumps. It gained success in 1996 and then extended applications. In the later 1990s, a few demonstration projects also appeared in Liaoyang, Liaoning province and Jinan, Shandong province. At that time, several universities carried out experimental studies including theoretical modes and testing applications (Diao and Fang, 2006). At the end of 2000, GSHP reached 100 thousand m^2 of application. GSHP systems started high speed growth when entering the 21st century. The application was 7.67 million m^2 in 2004 and 100.7 million m^2 in 2009. During this period, Shenyang exceeded Beijing and became the first place in the country in 2007. It occupied 54 percent of total application numbers in China. Hereafter, Shenyang decreased its high-speed for partial adjustment but still kept the top position.

However, GSHP shows a positive and favourable progress in the first decade of the 21st century, probably due to the serious haze problem in eastern China. So GSHP application accelerated again. A new trend shows the most rapid growth appeared in the mid down-stream regions of the Yellow River and Yangtze River where there had been no winter space heating in the past. For example, in Jiangsu province there was no space heating under the planning economy. But with winter air temperatures lower than 5°C, it needs space heating. Developers have constructed new buildings including GSHP systems in recent years, which the public has welcomed. Another example is in Wuhan city. The local government has initiated the 'warm in winter and cool in summer' project. Therefore, all new buildings will use GSHPs for heating in winter and cooling in summer. Existing buildings will be remoulded by GSHPs progressively.

Figure 5.1-2. Growth of Ground Source Heat Pumps in China

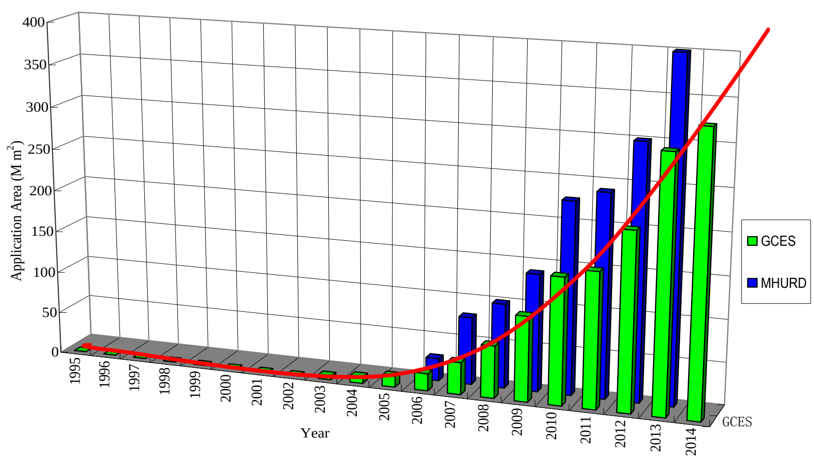

GSHP = geothermal source heat pump.
Source: Keyan Zheng et al (2015).

Figure 5.1-3. 20 Years' Growth of Geothermal Direct Use and Proportion of Ground Source Heat Pumps in China

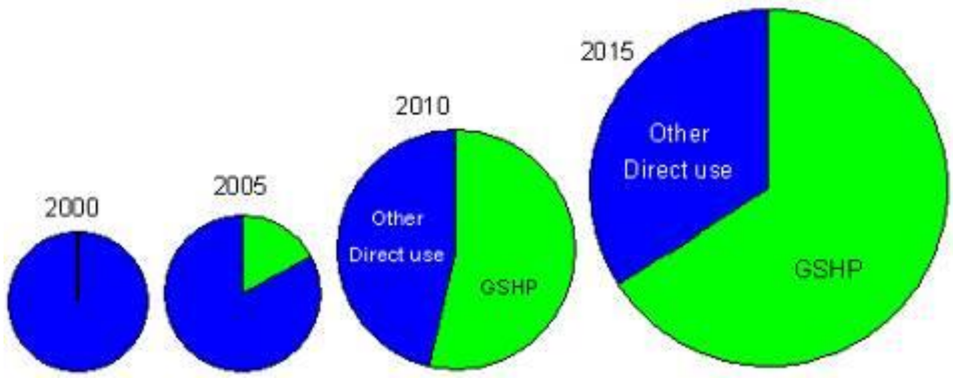

Notes: Area of circle = total direct use; green part = GSHP, GSHP = geothermal source heat pump.

Source: Edited by authors based on statistics data of the Geothermal Council of China Energy Society.

GSHP application reached 330 million m^2 in China in 2014. Its installed capacity will be 11.8 GWt with annual energy use of 110,311 terajoule per year (TJ/yr). GSHP application has a progressive annual increase rate of over 27 percent, higher than the rest of the world. **Figure 5.1-2** shows the process of GSHP growth in China. The long series shows the statistics from the Geothermal Council of China Energy Society (GCES); the short series shows the data from official website of the Ministry of Housing and Urban-Rural Development (MHURD), in which data consist of all heat pumps including industrial waste water and urban sewage.

For such a rapid growth, the primary reason is policy support from the national and local governments. The first is the Law of Renewable Energy of P. R. China and then a series of government documents. The Ministry of Housing and Urban–Rural Development and the Ministry of Finance jointly supported a series of projects on energy saving for buildings, including demonstration projects on demonstration county and smart city, amongst others.

5.1.2. Case Study 1: Shallow geothermal energy investigation and evaluation

The GSHP application may contain risk in inappropriate locations. In order to reduce such risks, the Ministry of Land and Resources has supported a huge project for 287 prefecture-level cities for investigation and evaluation of shallow geothermal energy, which is mainly organised by each province (region, city), promoted by the cooperation of the province and the Ministry of Land and Resources. The fund has spent for over CNY100 million (about US$16 million). The first demonstration was in Tianjin city to carry out the pilot work, and make uniform the methods and techniques. Secondly, based on the experiences obtained from the pilot work in Tianjin, this work spread to other cities. Based on the identification of shallow geothermal energy storage condition, reports and maps show the suitable, basic-suitable, and unsuitable areas for GSHP development. These achievements have been provided to local governments for application in further GSHP projects. **Figure 5.3-4** shows such results from the Beijing achievement. It indicates the best, good, and poor conditions (divisions) for GSHP application of water type and soil type respectively.

The national project of investigation and evaluation of shallow geothermal energy has shown great potential. It provides heat capacity for GSHP use. The total potential is equivalent to 9.486 billion tonnes of standard coal (Wang, et al., 2013).

Figure 5.1-4. Map Showing Shallow Geothermal Energy Conditions in Beijing

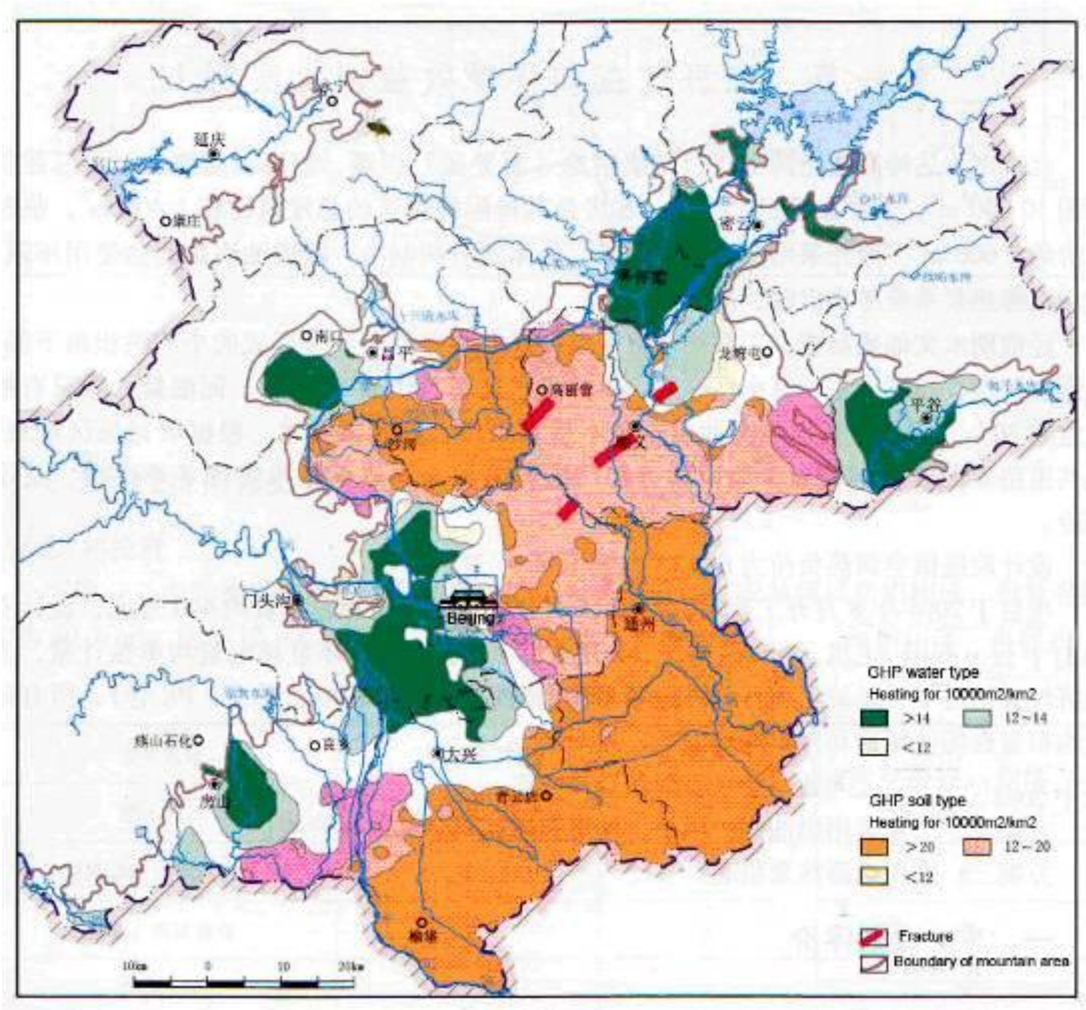

Source: Keyan Zheng et al. (2015).

5.1.3. Case study 2: Monitoring of ground temperature recovering

Construction designers worried about the balance of heating–cooling for GSHP application. Long-term monitoring has been carried out in typical projects for more than 10 years. By long-term monitoring of ground temperature and heat pump system, it has shown positive results. Similar results have come from 20 more projects in Beijing.

Figure 5.1-5. Installation of Monitoring Tools for Ground Source Heat Pump System

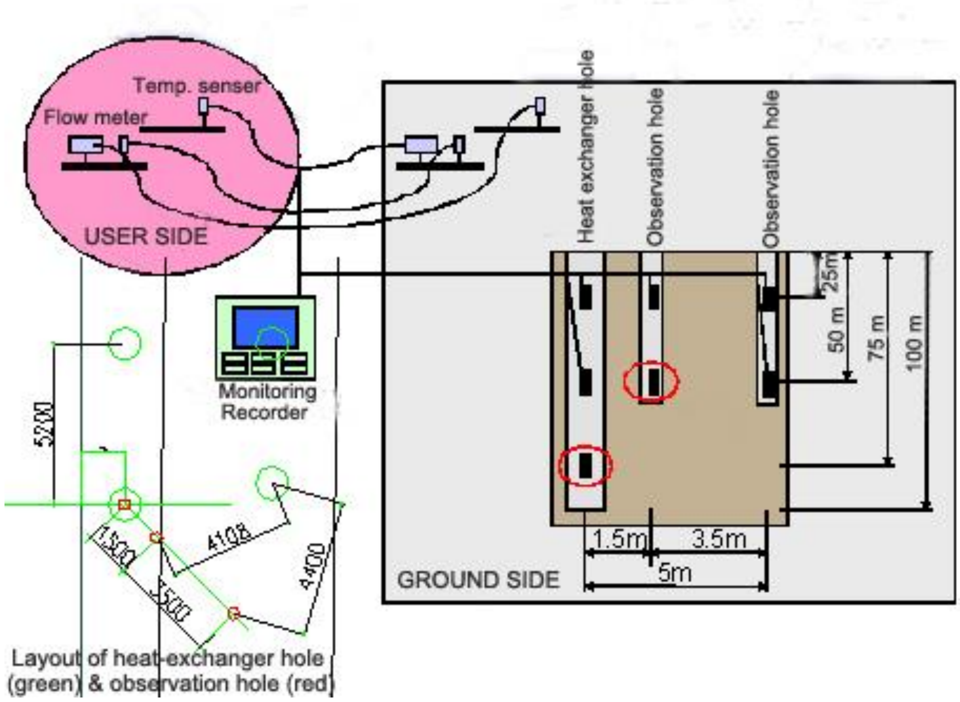

Source: Zhuang, Y. et al. (2010).

Figure 5.1-6. Temperature Curves Measured in Different Monitoring Holes

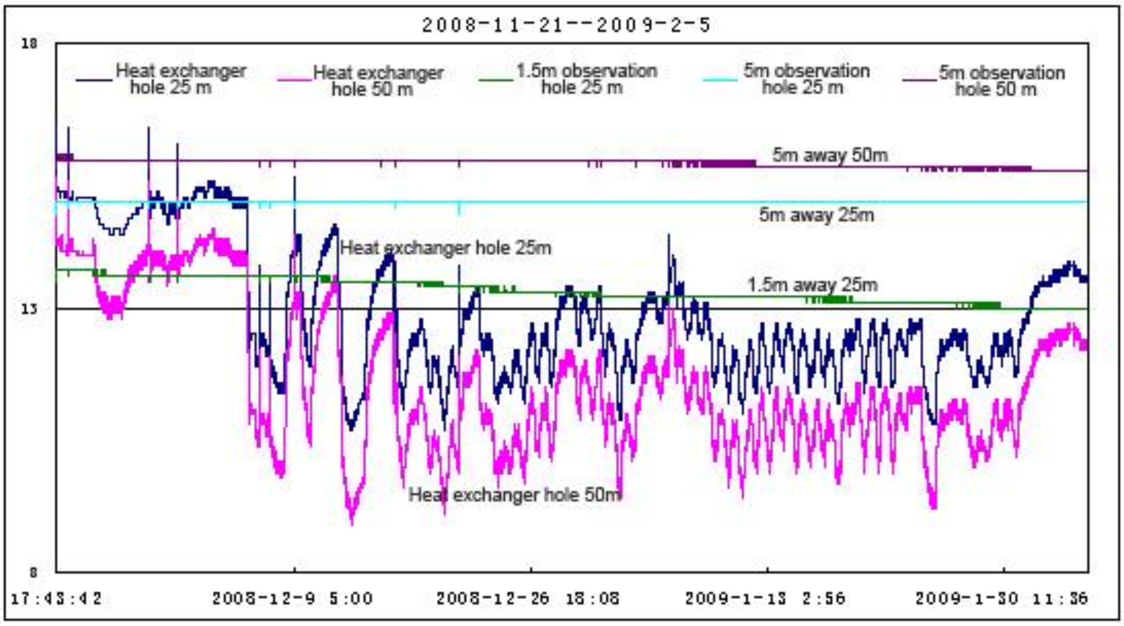

Source: Zhuang, Y, et al. (2010).

Figure 5.1-7. Geo-temperature Recovery During and After Heating Season

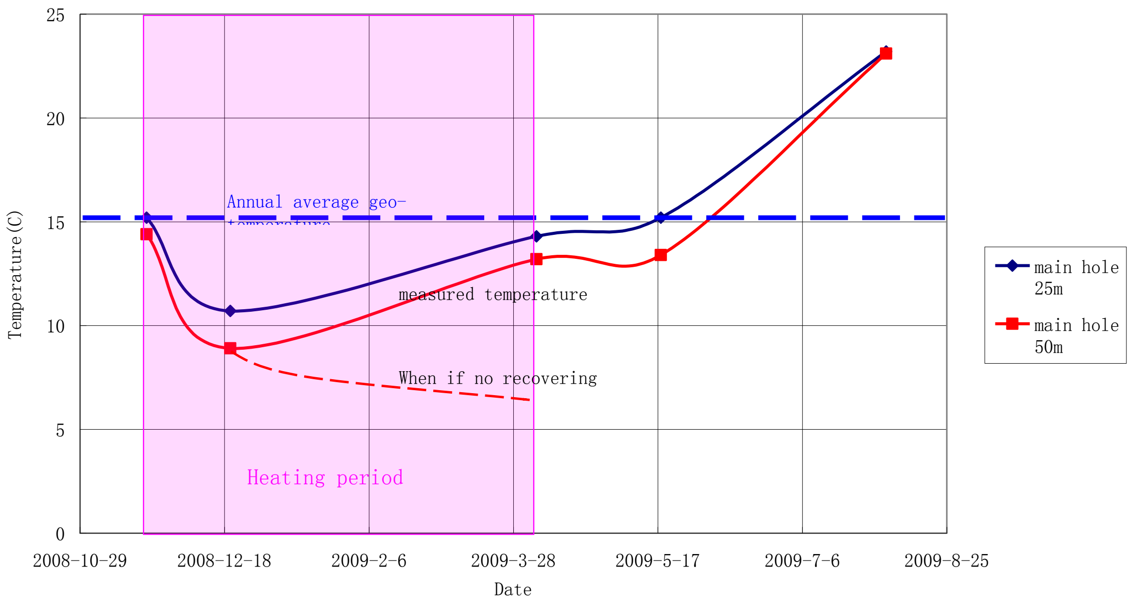

Source: Edited by authors based on monitoring data from Beijing Geothermal Engineering Institute.

Figure 5.1-8. Geo-temperature Recovery During and After Cooling Season

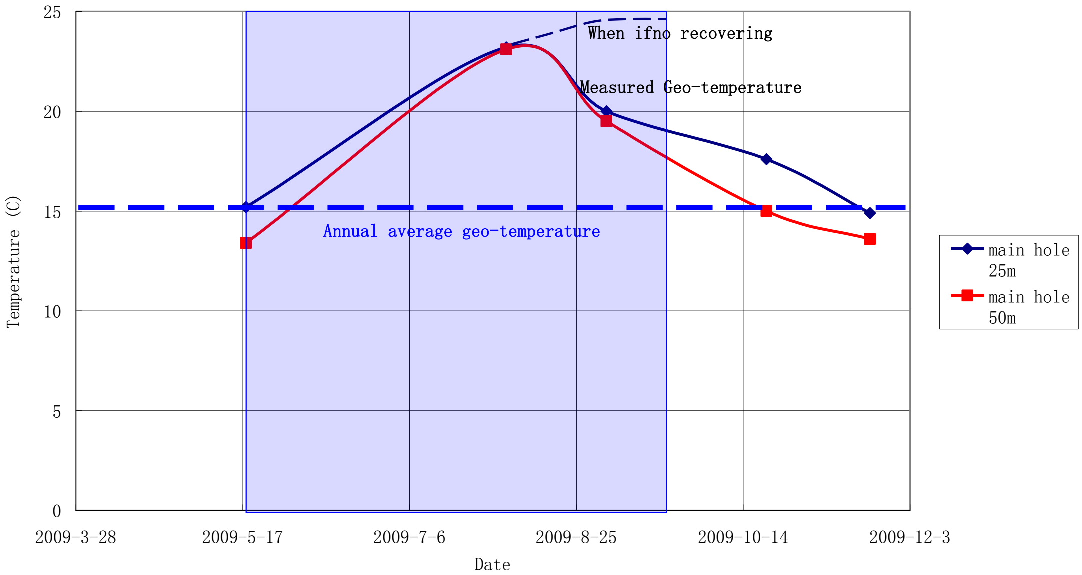

Source: edited by authors based on monitoring data from Beijing Geothermal Engineering Institute.

Lessons learned

- Mapping shallow geothermal energy conditions, such as water type and soil type, is important to perform proper design of GSHP systems.
- Monitoring of ground temperature is important to monitor thermal recovery of the ground and to assure the balance of heating and cooling.

References

Zheng. K., Y. Mo, L. Chen (2015), 'Twenty Years of Geothermal Heat Pump in China,' Proceedings of World Geothermal Congress 2015, 29025, p.4.

Zhuang, Y. et al. (2010), 'Study on Ground Temperature Variation of Heat Exchange Area of GSHP,' *Hydrogeology and Engineering Geology*, Vol.37, (6): 134–138 (in Chinese with English abstract).

5.2. Japan: Suitability Mapping for Both Closed Loop and Aquifer Thermal Energy Storage Systems

5.2.1. Suitability mapping for ground source heat pump application

Heat exchange rate and preferred drilling depth of a GSHP system varies with local hydrogeological settings in sedimentary basins and plains in monsoon Asia. Therefore, groundwater and geological surveys to perform numerical simulation on groundwater flow and local heat exchange are needed to compile suitability maps of GSHP systems (**Figure 5.2.1-1**). Design of the GSHP system can be improved by utilising the suitability map, such that high system performance and cost reduction may be achieved.

Figure 5.2.1-1. Potential Heat Exchange Rate in the Fukui Plain based on Simulation Results

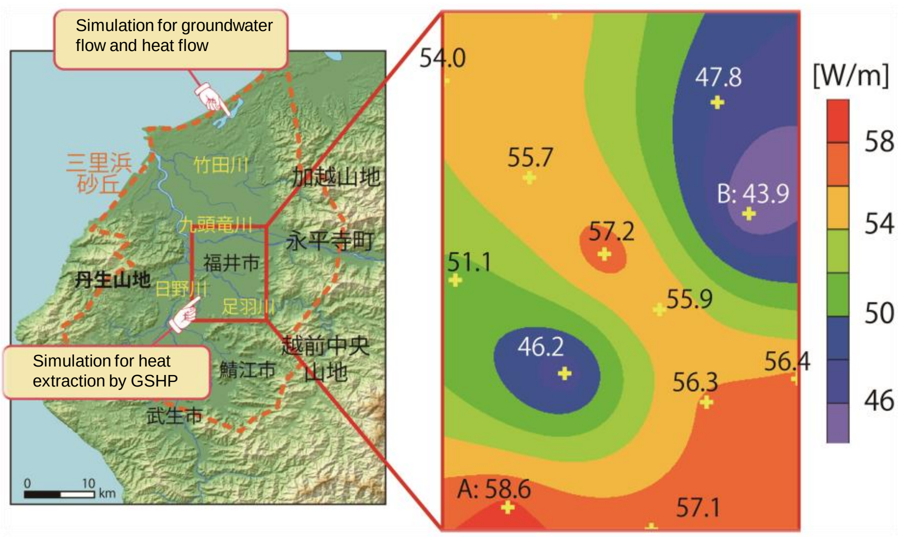

Source: Yoshioka, et al. (2010).

In general, there are two types of GSHP systems, closed-loop and open-loop systems (**Figure 5.2.1-2**). In a closed-loop system, the ground heat exchanger (GHE) with U-tube is installed in bore hole and heat transfer medium (anti-freezing liquid) is circulated in order to exchange heat with the subsurface. In an open-loop system, groundwater is directly used by pumping for heat exchange at ground surface and reinjected after heat exchange. It is said that the closed type can be used anywhere, while the use of the open type is limited to places where groundwater aquifer is present, preferably at shallow depth.

Figure 5.2.1-2. Types of Ground Source Heat Pump Systems

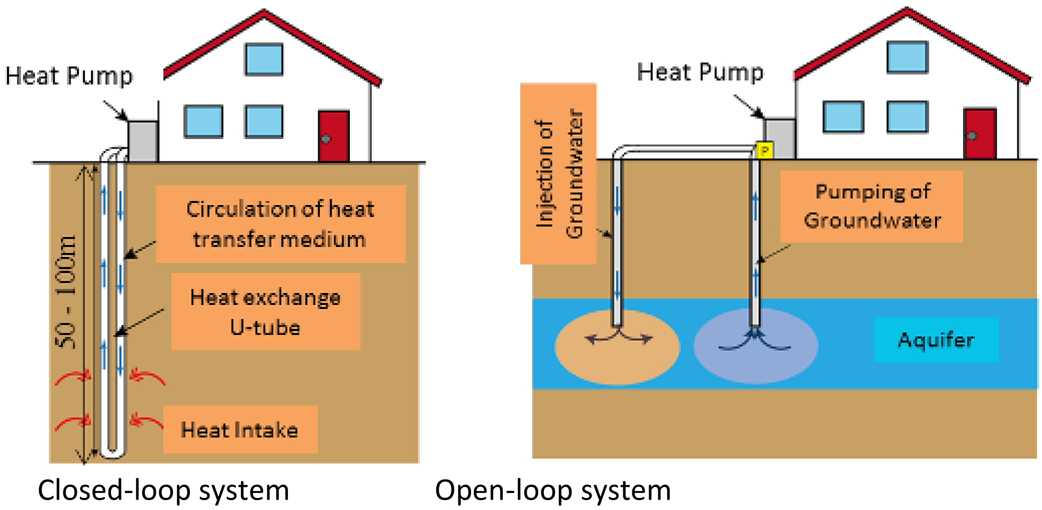

Source: Edited by the authors.

5.2.2. Case study 1: Suitability map for closed-loop GSHP system; development of suitability map for installation of GSHP system

5.2.2.1. Introduction

The objective of this study is to assess the installation suitability of a closed-loop GSHP system by developing 'suitability' maps. The term suitability is mainly related to heat exchange with the subsurface, which depends on geology, groundwater flow system, and subsurface temperature distribution. Hence, suitability assessment should be done based on hydrogeological and thermal information. The study area is the Tsugaru Plain situated in the western part of Aomori Prefecture, Japan (**Figure 5.2.2-1**).

5.2.2.2. Regional scale analysis model

For the assessment of usage possibility of ground source heat energy, groundwater flow system, and subsurface temperature distribution must be understood. For this purpose, a regional scale analysis model (**Figure 5.2.2-2**) was prepared using finite element code FEFLOW (Diersch, 2005). Model boundary was defined along dividing ridges surrounding the plain.

Figure 5.2.2-1. Tsugaru Plain with Model Boundary

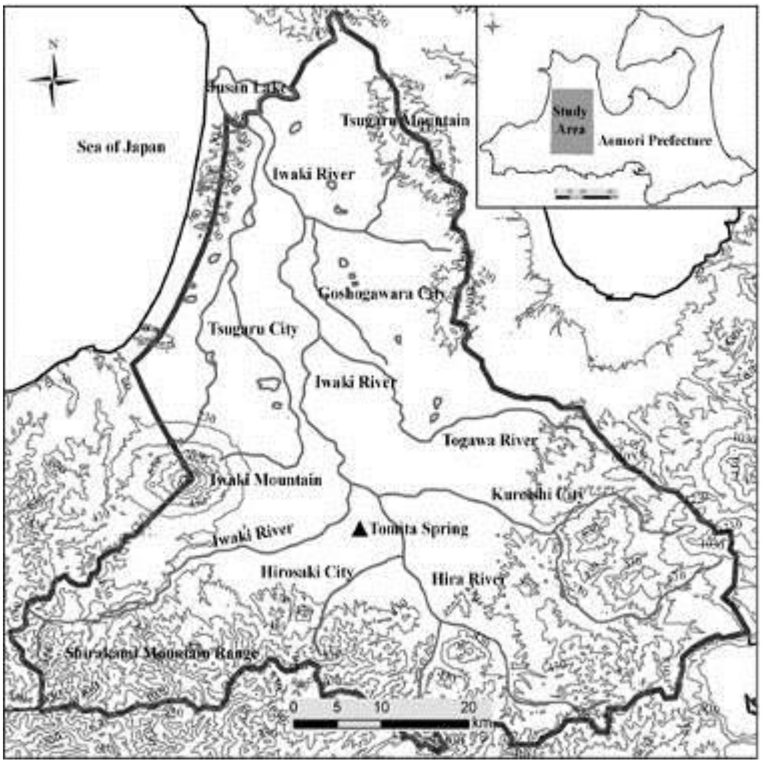

Source: Shrestha, et al. (2015).

Figure 5.2.2-2. Regional Scale Analysis Model of Tsugaru Plain

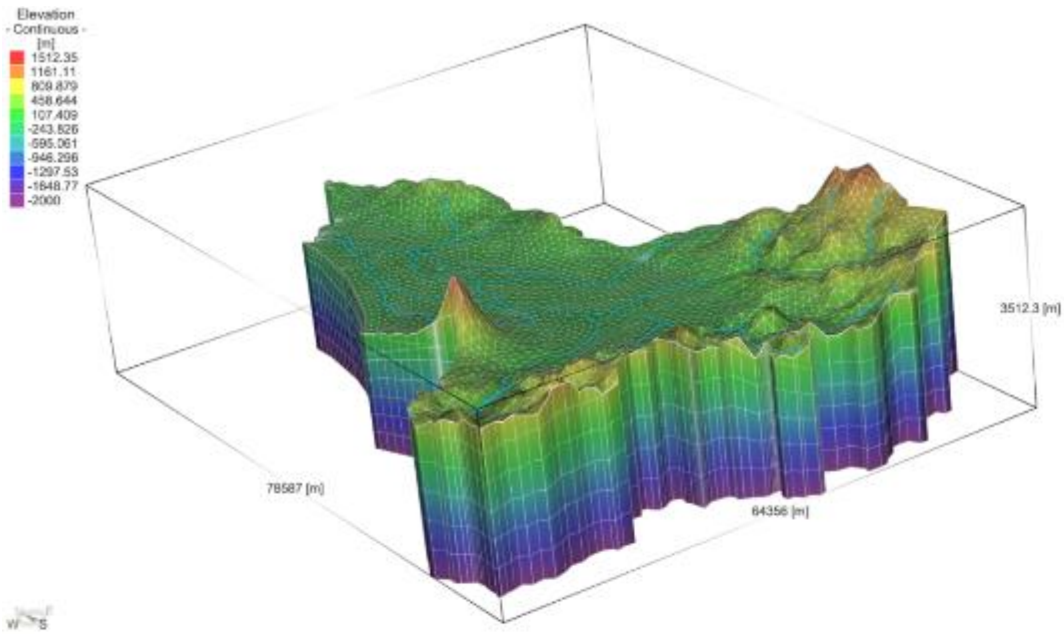

Source: Shrestha, et al. (2015).

Horizontal dimensions of the model were 64km and 78km in east-west and north-south directions respectively. In the model, layers 1 to 4 belonged to Quaternary System. Layers 5 to 7 belonged to Neogene and layers 8 to 12 belonged to Paleogene, both of which correspond to Tertiary System. Basal elevation of these geological layers were referred from Koshigai, et al. (2011). Quaternary System hosts the main aquifers of the Tsugaru Plain where groundwater flow primarily occurs.

Parameters adopted for the geological layers are shown in **Table 5.2.2-1**. Hydraulic conductivities of geological layers were determined by trial and error method based on the comparison of simulation results with the data of past studies and by confirming the path of simulated groundwater flow.

Regarding thermal conductivity, it was set by matching the results of single ground heat exchanger (GHE) model and thermal response test (TRT) which will be explained later.

Table 5.2.2-1. Model Parameters at Natural Springs and Lakes

	Quaternary System	**Tertiary System**	
		Neogene	Paleogene
Hydraulic Conductivity (m/s)	5×10^{-5}	3.4×10^{-6}	2.4×10^{-7}
Porosity (-)	0.4	0.1	0.1
Heat Capacity (J/m^3K)	2.6×10^{6}	2.6×10^{6}	2.6×10^{6}
Thermal Conductivity (W/mK)	1.2	1.5	1.5

Source: Shrestha, et al. (2015).

5.2.2.3. Groundwater flow and heat transport simulation

With this regional-scale analysis model, saturated steady state simulation of groundwater flow and heat transport was conducted. Regarding boundary conditions of the groundwater flow system, the top of the model was fixed by the water table that was determined as a function of surface elevation. The bottom of the model was treated as an impermeable boundary and the lateral sides were set as no flow boundaries. For boundary conditions of heat transport, the top and bottom of the model were fixed by time constant temperature boundaries, and lateral sides were set as adiabatic allowing heat transfer by groundwater convection only. The temperature distribution at the model top was estimated on the basis of the annual average temperature at Goshogawara City of

10.5°C and assuming a decrement rate in ambient temperature with elevation of 0.7°C/100m. The temperature distribution at the bottom was estimated based on the surface temperature distribution, using a geothermal gradient of 3°C/100m (GSJ, 2004).

In the absence of measured hydraulic heads of observation wells, computed results of the groundwater flow system were indirectly verified by comparing them with results of past studies and literature values. At Hirosaki City located in the southern part of the plain, the calculated hydraulic head was in the range of 30 m. The hydraulic head presented by Sakai (1960) in that city was also around 30 m. Similarly, at a high school in Kuroishi City located in the southeast part of the plain, the calculated hydraulic head was 47.1m. The hydraulic head measured by Machida and Yasukawa (2008) in the same area was 47 m, very close to the calculated value. The depth of the water table from the ground surface was found to be shallow in most areas of the plain. Machida and Yasukawa (2008) and Aomori Prefecture (2011) also showed similar results, implying the sustainable operation of GSHP systems in terms of groundwater availability and saturation of geological layers.

Natural water bodies such as springs, lakes, and ponds are generally formed by the upflow of groundwater. Simulation results were further validated by inspecting the path of simulated flow at natural water bodies, confirming if the groundwater was flowing in an upwards direction. At Tomita Spring located in Hirosaki City, the groundwater was found to be flowing in an upwards direction (**Figure 5.2.2-3**). Likewise, upflow was also found at other natural lakes and ponds. It can be said that the calculated results of the groundwater flow were consistent with the natural conditions and data of past studies.

Figure 5.2.2-3. Groundwater Upflow at Tomita Spring

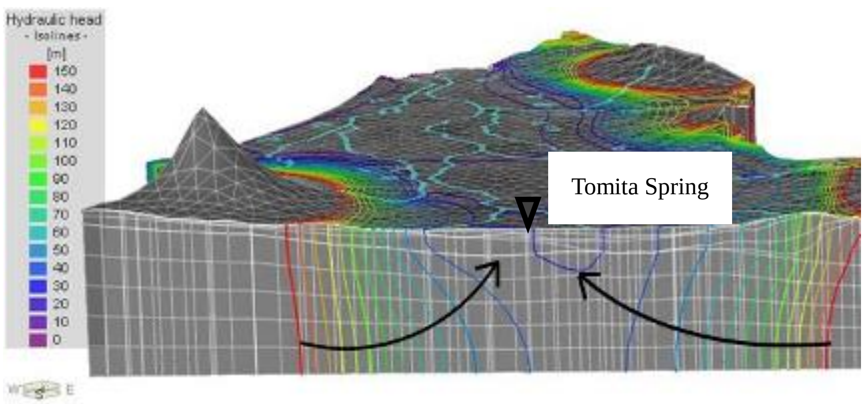

Source: Shrestha, et al. (2015).

5.2.2.4. Single ground heat exchanger model

Subsurface temperature distribution computed from the regional-scale analysis model could not be verified with measured vertical temperature profiles because observation wells were lacking. Hence, to verify the analysis model and its results, single GHE models were constructed at eleven locations (**Figure 5.2.2-4**), where TRT had been conducted. Single GHE models of dimensions 20 m x 20 m x 100 m were developed using the finite element software FEFLOW. Data related to TRT were referred from Aomori Prefecture (2011) and Kuroishi City (2011). Thermal conductivities of geological layers were determined by matching the results of GHE models with those of TRT.

Figure 5.2.2-4. Single Ground Heat Exchanger Model and Locations of Thermal Response Tests

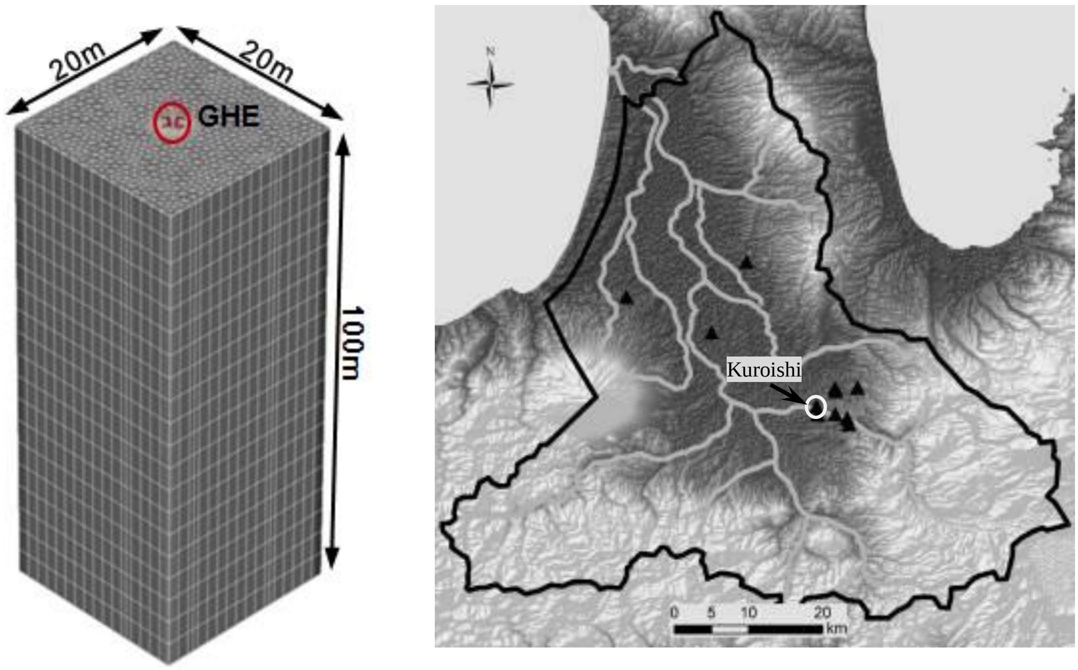

Notes: Single ground heat exchanger model (left) and locations of thermal response tests and single ground heat exchanger models (right).
Source: Shrestha, et al. (2015).

In TRT, 50 m deep GHE was used which contained single U-tube of outer diameter 0.034 m. TRT was conducted by applying heat load of 3 kW to heat transfer medium (water), which was circulated for about 2 days at the rate of 20 litter per minute (L/min). Geological data and hydrological parameters assigned to each GHE model were adopted from their corresponding locations in the analysis model. At the center of GHE model, 50 m deep GHE was installed (**Figure 5.2.2-4**).

Regarding boundary conditions of groundwater flow system, top and bottom of the GHE model were set as no flow boundaries. Lateral sides were fixed with hydraulic heads to reproduce groundwater velocity, which was resulted in the analysis model at the corresponding location. For boundary conditions of heat transfer, constant temperature boundary condition was applied to the top and bottom of the model. At the top, the same value as assigned in the analysis model was set, while the bottom was fixed with temperature distribution obtained from the analysis model. At the upstream lateral side from where groundwater flowed, a constant background temperature was assumed. Remaining lateral sides were set as adiabatic, allowing heat transfer by groundwater convection only.

For heat exchange simulation, temperature of the heat transfer medium at the inlet of GHE and its flow rate observed during TRT were taken as input parameters. As an output, temperature of the heat transfer medium at the outlet of GHE resulted from the simulation. Then, computed outlet temperature distribution with time was compared with the real time result of TRT to find whether they matched with each other (**Figure 5.2.2-5**). **Figure 5.2.2-5** shows that computed profiles of outlet temperature of the heat transfer medium were almost consistent with those observed during TRT. At other locations also, there was satisfactory agreement between computed and observed outlet temperature of the medium. In this way, the thermal conductivities of geological layers were determined and the constructed 3D regional-scale analysis model was verified.

5.2.2.5. Development of suitability maps for GSHP system

Groundwater flow and geological condition strongly affects heat exchange rate of GHE. Hence, suitability maps should be prepared based on hydrogeological and thermal information. For this purpose, thematic maps of groundwater velocity, subsurface temperature, water table depth, and sand-gravel ratio in geological layers were prepared using the Geographic Information System (GIS) (**Figure 5.2.2-6**). Groundwater flow velocity, subsurface temperature, and sand-gravel ratio were taken as average value up to 50 m depth from the surface.

Figure 5.2.2-5. Comparison of Computed and Observed Outlet Temperature of Heat Transfer Medium

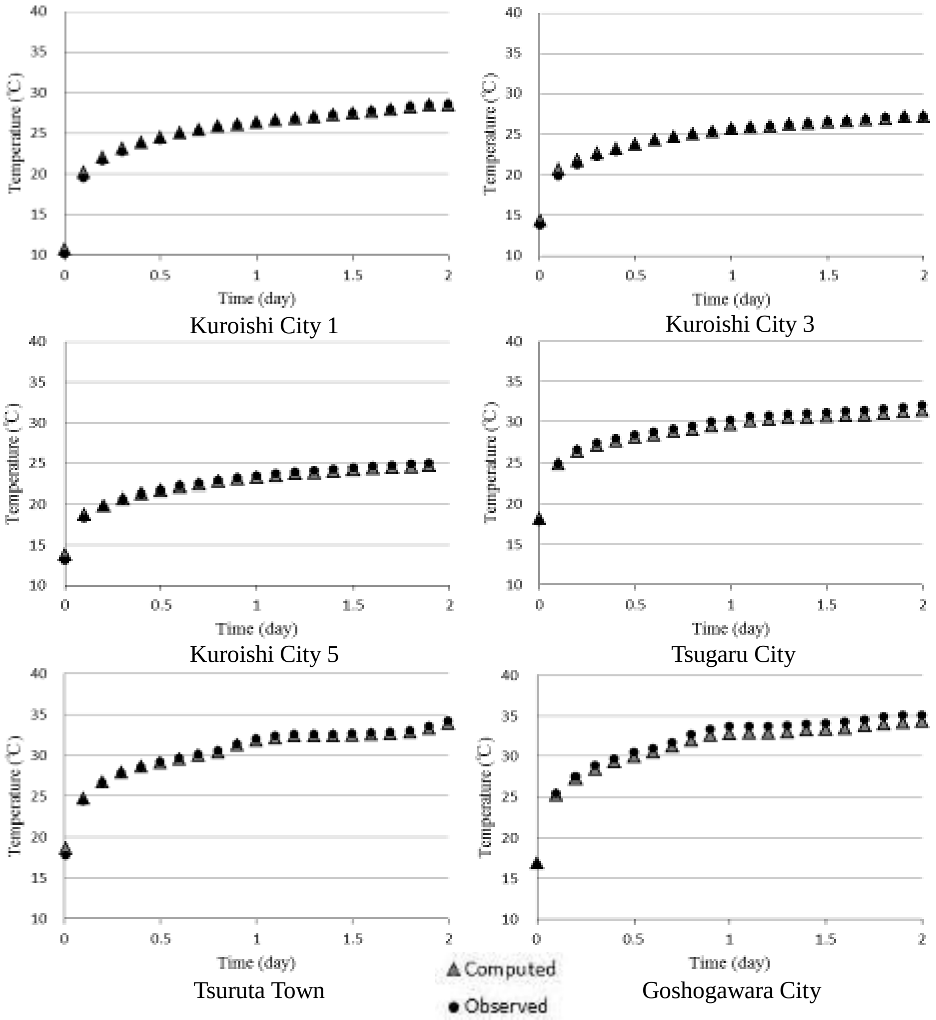

Source: Shrestha, et al. (2015).

Figure 5.2.2-6. Thematic Maps of Tsugaru Plain

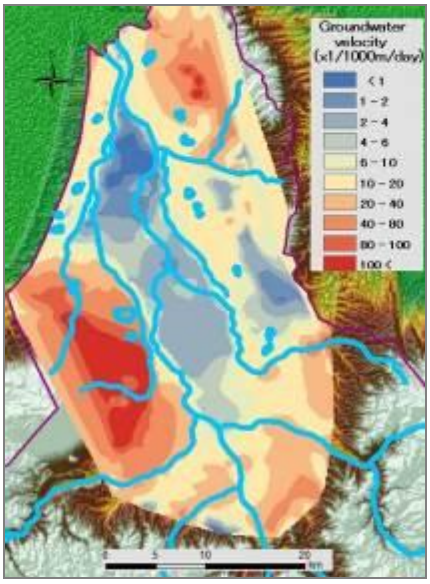

(a) Groundwater velocity

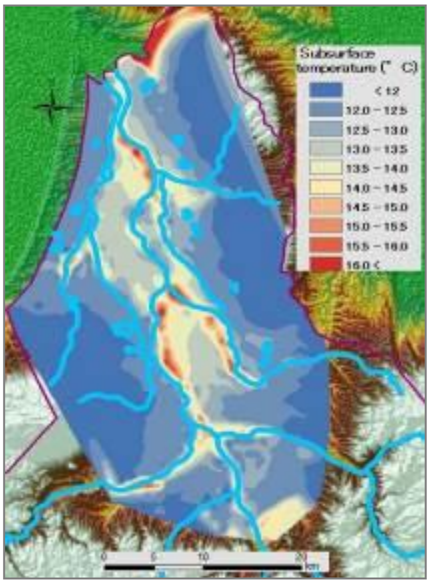

(b) Subsurface temperature

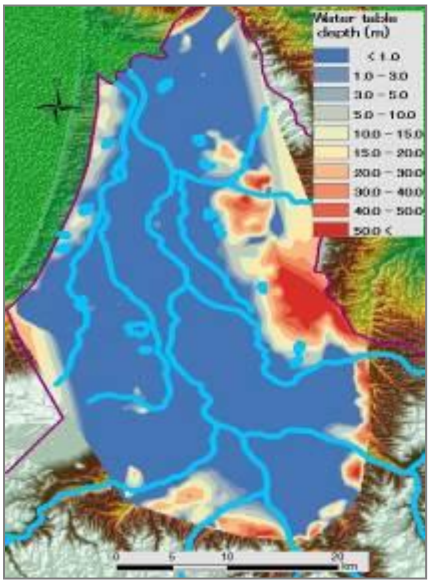

(c) Water table depth

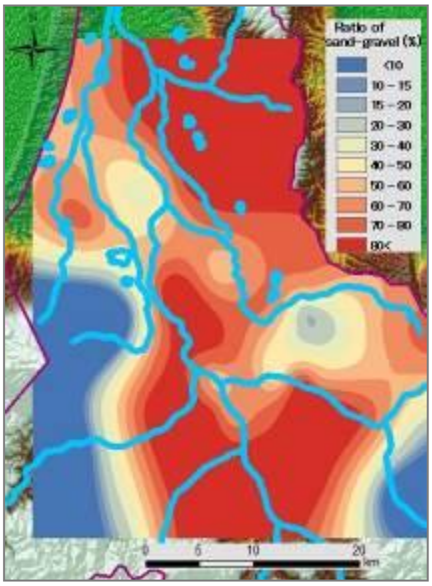

(d) Sand-gravel ratio

Source: Shrestha, et al. (2014)

Table 5.2.2-2. Reclassification of Thematic Maps

Groundwater velocity Index class (x 10^{-3}m/day)	Sand-gravel ratio Index class (%)	Water table depth from surface Index class (m)	Grade
< 1	<10	50 <	1
1 – 2	10 – 15	40 - 50	2
2 – 4	15 – 20	30 - 40	3
4 – 6	20 – 30	20 - 30	4
6 – 10	30 – 40	15 - 20	5
10 – 20	40 – 50	10 - 15	6
20 – 40	50 – 60	5 - 10	7
40 – 80	60 – 70	3 - 5	8
80 – 100	70 – 80	1 - 3	9
100 <	80 <	< 1	10

Source: Shrestha, et al. (2014).

In this study, a suitability map for space-heating and space-cooling purposes was prepared by overlaying the thematic maps in GIS using an overlay model (**Figure 5.2.2-7**). For overlaying, the parameter of each map was reclassified into index classes and each index class was assigned a grade ranging from minimum 1 to maximum 10 (**Table 5.2.2-2**). The higher the grade, the higher the suitability for the GSHP system. For space-heating and space-cooling, the subsurface temperature was not considered in the overlay model. The reason is higher and lower subsurface temperatures both are equally important for space-heating and space-cooling. Weightage was set for thematic maps, 35 percent for groundwater velocity, 35 percent for sand-gravel ratio, and 30 percent for water table depth. The weightage was set based on the variation of each parameter. Maps were overlaid based on grades applied to each cell and weightage assigned to each maps, resulting in the suitability map (**Figure 5.2.2-8**).

Figure 5.2.2-7. Overlay Model for Space-Heating and Space-Cooling

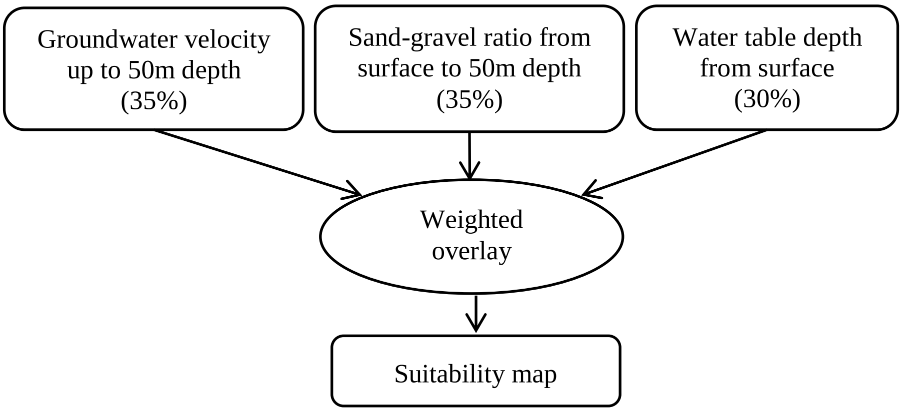

Source: Shrestha, et al. (2014).

Figure 5.2.2-8. Suitability Map of Tsugaru Plain

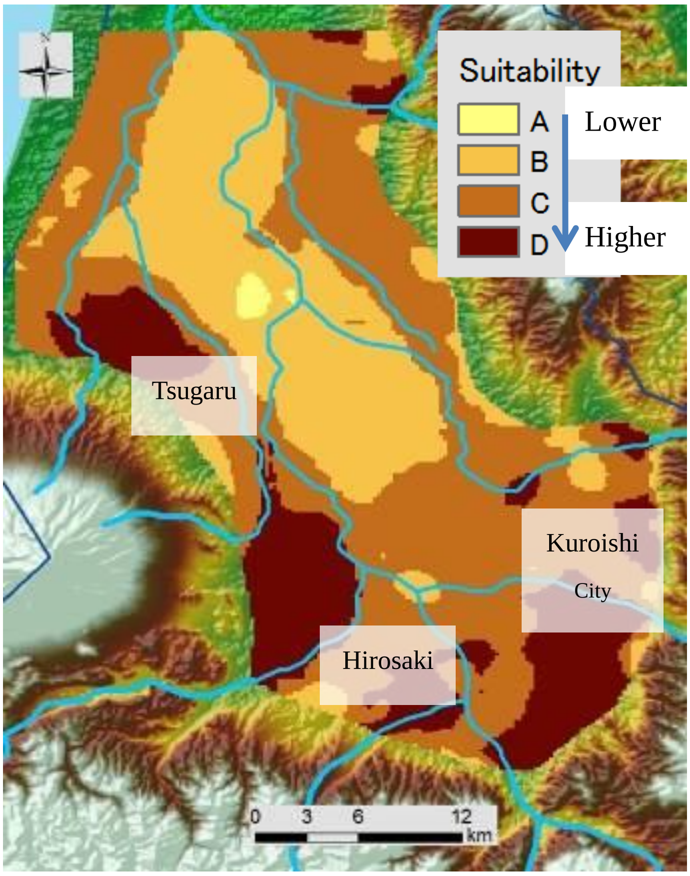

Source: Shrestha, et al. (2014).

In the legend of the suitability map, ranking A to D represent lower to higher suitability respectively for the installation of GSHP system. Suitability was found higher at the upstream and peripheral areas of the plain as compared to the central and downstream areas. Lower suitability does not mean that GSHP system cannot be installed.

It can be installed but longer length of GHE may be required and hence the higher cost. Major city areas such as Tsugaru City and Hirosaki City showed higher suitability with favourable geological and hydrological conditions. This kind of map that illustrates the variation of suitability is essential to adopt appropriate locations for the optimum design of the GSHP system.

5.2.2.6. Conclusion

The groundwater flow system and subsurface temperature distribution of Tsugaru Plain were comprehended by developing a regional scale analysis model. Hydrological and thermal data to the plain could not be measured as observation wells were lacking. However, the analysis model could be verified by constructing single GHE models and incorporating the results of TRT conducted in the field. Prepared thematic maps of groundwater velocity, subsurface temperature, water table depth, and sand-gravel ratio showing the variation of their respective parameters can be regarded as significant for the proper siting of the GSHP system. Suitability maps developed can be used to determine appropriate locations for space-heating and space-cooling purposes.

References

Aomori Prefecture (2011), 'Survey Report on Potential Use of Ground-coupled Heat Pump System and Hot Spring Temperature in Aomori Prefecture', Aomori, Japan.

Diersch, H.-J.G. (2005), *FEFLOW Reference Manual*. Berlin, Germany: WASY GmbH Institute for Water Resources Planning and Systems Research.

Geological Survey of Japan (2004), 'Geothermal Gradient and Heat Flow Data in and around Japan, Digital Geoscience Map P-5', AIST, Japan (CD-ROM version).

Koshigai, M., A. Marui, N. Ito, T. Yoshizawa (2011), 'Development of Three Dimensional Hydrogeological Model and Estimation of Groundwater Storage in Japanese Islands', *Journal of Japanese Association of Groundwater Hydrology,* 53(4), pp.357–377 (in Japanese with English abstract).

Machida, I., and K. Yasukawa (2008), 'Regional Groundwater Survey for the Use of Ground-coupled Heat Pump System in Aomori Prefecture', in *Aomori Prefecture, Vision for the Promotion of Ground-coupled Heat Pump System in Aomori Prefecture, Aomori, Japan*, pp.91–126 (in Japanese).

Sakai, G. (1960), Study on Hydrogeology and Groundwater of Hirosaki City (I). Hirosaki City, Japan, (in Japanese).

Shrestha, G., Y. Uchida, M. Yoshioka, H. Fujii, and S. Ioka (2014), 'Estimation of Suitable Locations for Ground-source Heat Energy Use in Regional Scale', 2014 Annual Meeting, Geothermal Research Society of Japan, Abstracts with Programs, Akita, Japan.

Shrestha, G., Y. Uchida, M. Yoshioka, H. Fujii, and S. Ioka (2015), 'Assessment of

Development Potential of Ground-coupled Heat Pump System in Tsugaru Plain, Japan. *Renewable Energy,* 76, pp.249–257.

Yoshioka, M., Y. Uchida, Y. Yoda, H. Fujii, and S. Miyamoto, S. (2010), ‘Adoption of Suitability Area for Ground-coupled Heat Pump System 2nd Paper, Development of Heat Exchange Rate Maps using Groundwater Flow/Heat Transport Modeling’, *J. Geotherm. Res. Soc. Japan,* 32(4), pp.241–251 (in Japanese with English abstract).

5.2.3. Case study 2: Suitability map for open loop GSHP system; Groundwater flow and heat transport modelling to estimate the area suitable for aquifer thermal energy storage

5.2.3.1. Introduction

An aquifer thermal energy storage (ATES) system is one of the most energy-saving heating and cooling systems that utilises open-loop shallow geothermal technology (**Figure 5.2.3-1**). Development of this system is still limited in Japan because of the complex hydrogeological conditions. For promotion and sustainable utilisation of an ATES system, it is important to evaluate areas suitable for the system, especially in terms of hydrogeology. The purpose of this study is to estimate the area suitable for an ATES system using large-scale groundwater flow and heat transfer modelling.

The study area is Yamagata Basin (**Figure 5.2.3-2**) located in the central region of Yamagata Prefecture, Japan. It extends about 35 kilometres (km) from north to south and 15 km from east to west.

Figure 5.2.3-1. Aquifer Thermal Energy Storage System

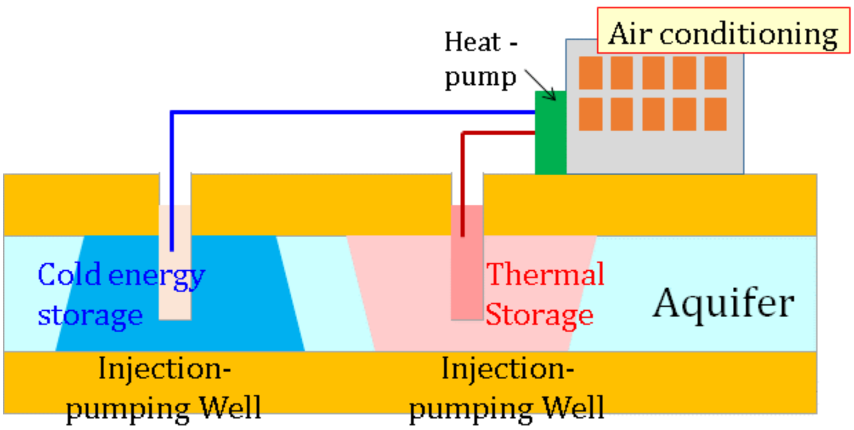

Source: Edited by authors.

5.2.3.2. Regional-scale groundwater flow and heat transport modelling

3D groundwater flow and heat transport modelling of Yamagata Basin was conducted using FEFLOW. The model boundary is shown in **Figure 5.2.3-2**. Southern and eastern boundaries of the target area were defined along dividing ridges. Northern and western boundaries were decided by considering the local geography because there were no dividing ridges. 3D analysis model (**Figure 5.2.3-3**) consists of 7 layers in the Quaternary System and 11 layers in the Neogene System. The bottom elevation of Quaternary System was decided by using 'Basement of Quaternary maps in Japan' (Koshigai, et al., 2011). The hydraulic and thermal properties of geological layers are shown in **Table 5.2.3-1**.

Figure 5.2.3-2. Yamagata Basin with Model Boundary

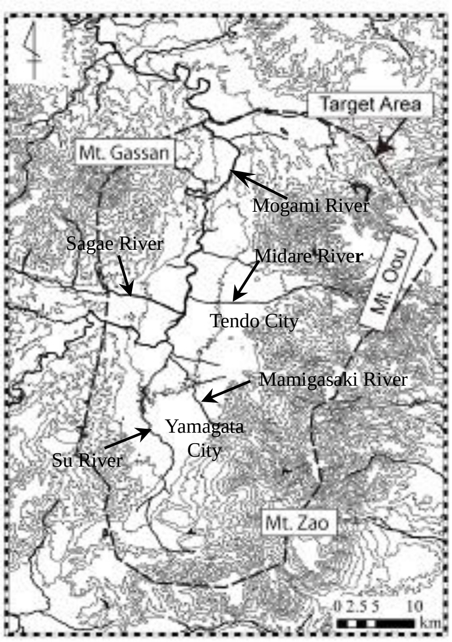

Source: Yoshioka et al. (2012).

Figure 5.2.3-3. 3D Analysis Model of Yamagata Basin

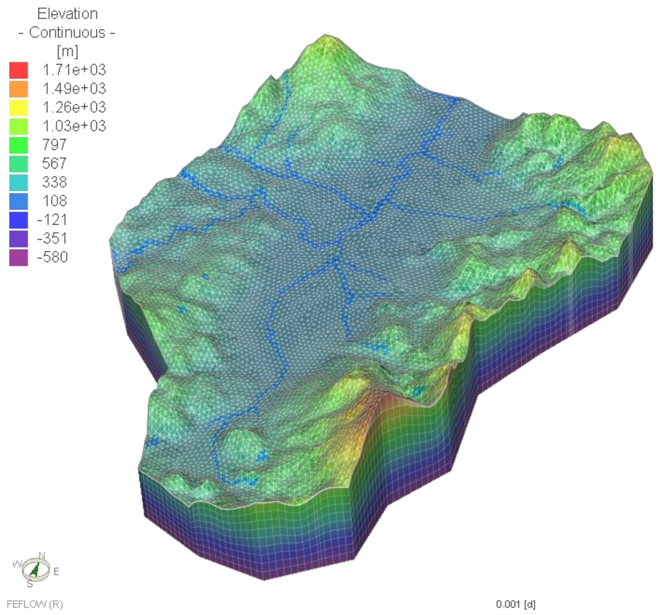

Source: Yoshioka et al. (2012).

Table 5.2.3-1. Physical Properties Used in the Analysis Model

	Unit	Quaternary (1–7 layers)	Neogene (8–18 layers)
Hydraulic conductivity (k_x, k_y)	m/s	7.6e-5	2.2e-8
Hydraulic conductivity (k_z)	m/s	7.6e-6	2.2e-9
Porosity	-	0.2	0.1
Dispersion Length	m	Longitudinal: 100, Transverse: 10	
Heat Capacity	J/kgK	2.6e6	
Heat Conductivity	W/mK	2.0	1.5

m/s = metre per second, m = metre, J/kgK = joule per kilogram Kelvin, W/mK = watt per metre Kelvin.
Source: Yoshioka et al. (2012).

The hydraulic and thermal properties of geological layers are shown in **Table 5.2.3-1**. Hydraulic properties (for example, hydraulic conductivity and effective porosity, amongst others) were decided using the previous studies (GSJ, 2012; Tohoku Regional Office, 1994).

Regarding boundary conditions of groundwater flow, the lateral sides of the model were fixed with a time-constant hydraulic head, which was determined as a function of surface elevation. At the northern and western sides of the basin, it was difficult to select the model boundary along dividing ridges. Therefore, pre-calculation was done using larger scale groundwater flow modelling, which included most of Mogami River and surrounding mountains. Hydraulic heads resulting from the pre-calculation were used as the boundary conditions. The top of the model was also set as time-constant hydraulic head boundary and the bottom was set as no flow boundary. For heat transport, the top and bottom of the model were fixed with time-constant temperature boundaries, and the lateral sides were set as no heat flow boundaries. Temperature distribution at the model top was estimated based on the average air temperature of Yamagata City and assuming a decrement rate in ambient temperature with elevation of 0.65°C/100m. Temperature distribution at the model bottom was estimated based on temperature distribution at the model top, using a geothermal gradient (GSJ, 2004).

5.2.3.3. Results of groundwater flow – heat transport model

Figure 5.2.3-4 shows the distribution of the calculated hydraulic head, measured groundwater level and their comparison. According to the previous studies in this basin, at the top of Mamigasaki River's alluvial fan, the elevation of groundwater level was about 200 m, at the southern edge it was about 150 m, and around the centre the elevation was about 90 m. It was determined that the calculated results were in agreement with measured values.

In order to verify the calculated subsurface temperature distribution, measured subsurface temperature profiles were used. Subsurface temperature profiles were measured at 20 points in Yamagata Basin (GSJ, 2012). A digital thermistor with 300 m cable was inserted into observation wells and groundwater temperature was measured at 2 m depth intervals. **Figure 5.2.3-5** shows the distributions of measured and calculated subsurface temperature at 50 m depth from surface.

Figure 5.2.3-4. Distribution of (a) Calculated Hydraulic Head, (b) Measured Groundwater Level, and (c) Comparison of Calculated and Measured Values

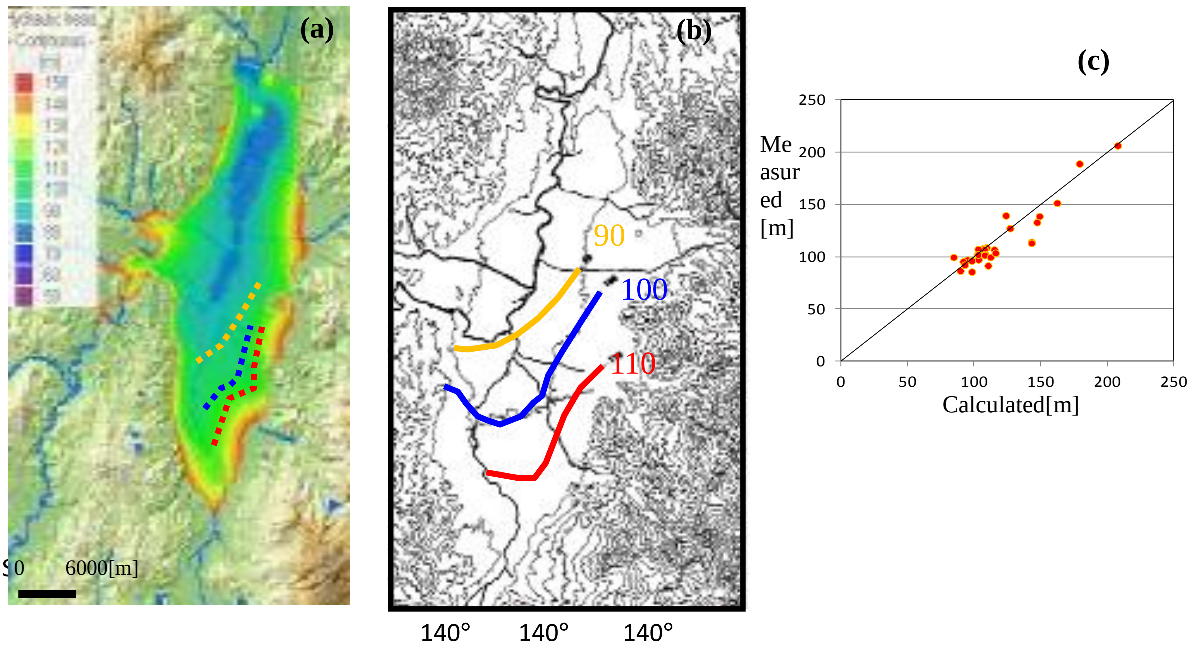

Figure 5.2.3-5. Distribution of Subsurface Temperature at a Depth of 50 Metres

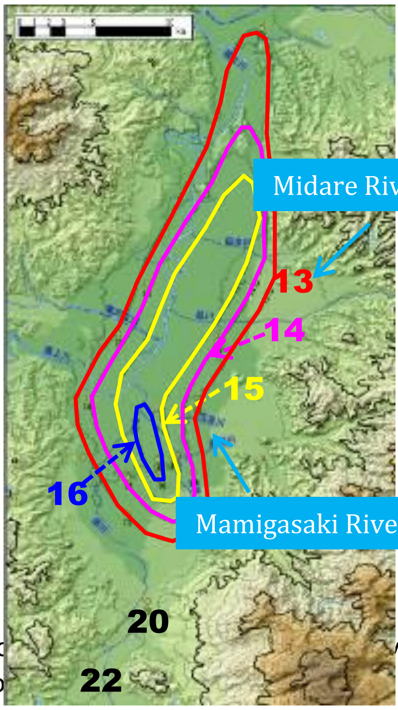

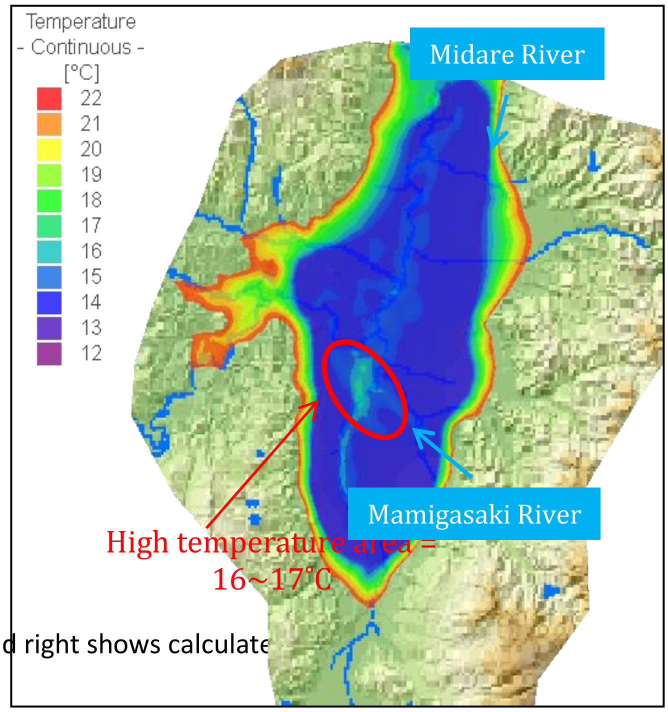

Nc values and right shows calculate
So

In both figures, the similar tendency of temperature distribution was found, that is, the temperature at the centre of the basin is higher than surroundings and the higher temperature zone elongates from the centre to the north along the Mogami River. The subsurface temperature is influenced not only by heat flux from the deep underground, but also advection due to groundwater flow. In general, the subsurface temperature in the recharge area is lower and that in the discharge area is higher at the same depth (Domenico and Palciauskas, 1973). The measured and calculated subsurface temperature cross-section views are shown in **Figure 5.2.3-6**. The convex form of the temperature profile can be seen in both figures and this area corresponds to the discharge area.

Figure 5.2.3-6. Subsurface Temperatures along Cross-section A-A’

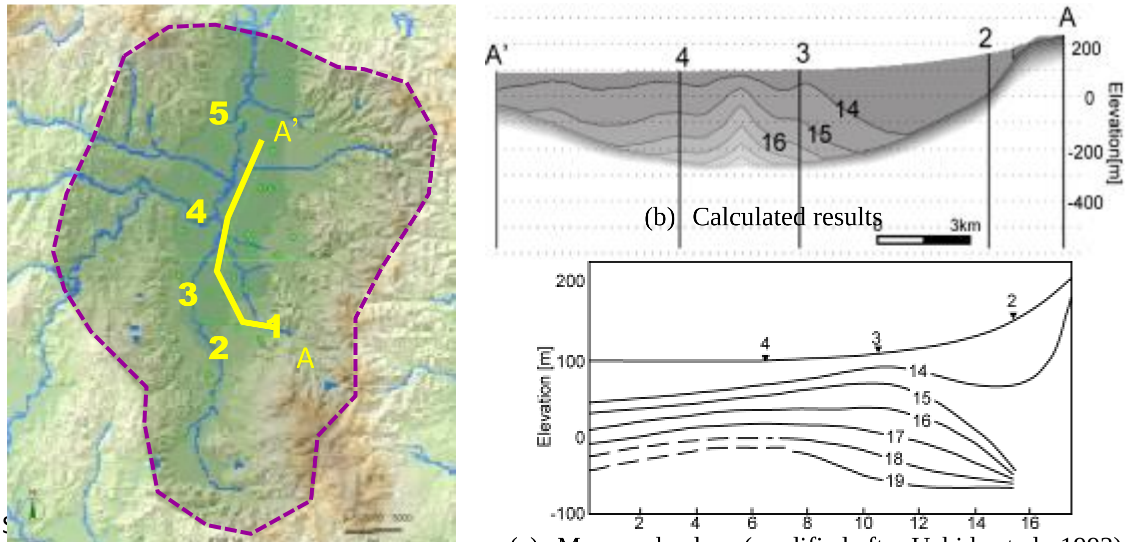

(b) Calculated results

(a) Measured values (modified after Uchida et al., 1993)

5.2.3.4. Indicative parameters for the suitability analysis of ATES system

Areas suitable for the ATES system depend on hydrogeological conditions. For example, pumping capacity is regulated by groundwater availability and hydraulic conductivity, whereas the ability of thermal storage depends on groundwater flow. In this study, parameters that can influence the system performance (called ‘indicative parameters’ hereafter) are adopted. Their values were obtained from the results of the regional-scale modelling and used for the evaluation of areas suitable for the ATES system in the Yamagata Basin. Indicative parameters considered are as follows.

- Horizontal groundwater flow:

It is most important for the ATES system to evaluate the horizontal groundwater flow velocity because the stored thermal energy in an aquifer may be transferred by groundwater flow in faster groundwater flow regions.

- Vertical groundwater flow:

Downward flow of groundwater occurs in recharge areas, which is considered to be applicable for an ATES system. On the other hand, upward flow occurs in discharge areas, which is a drawback for the system because the pumped groundwater cannot be reinjected in these areas.

- Geological setting:

The availability of groundwater and the effect of pumping to the surrounding environment (for example, land subsidence) are controlled by hydrogeological parameters, especially hydraulic conductivity. The higher the hydraulic conductivity, the higher the amount of groundwater can be pumped in general. However, it is site specific.

Hydraulic conductivity varies with the geology. Hence, the geological setting was considered as an indicative parameter in this study.

The groundwater level was found to be higher throughout the basin. For groundwater quality, there were no experimental results. Regarding the subsurface temperature, both low and high temperatures are important for the system. With these reasons, the above mentioned three parameters were taken as indicative parameters in this study. For each of these parameters, weightage was assigned to assess the suitable area for the system.

Weightage of geological setting (W_g):

The weightage of the Quaternary System was assumed to be 1 and that of the Neogene System as 0. This is because the hydraulic conductivity of the Quaternary System is higher than that of the Neogene System by about 3 order. The permeable layer makes it easier to pump up groundwater.

Weightage of horizontal groundwater velocity (W_h):

The weightage of horizontal groundwater velocity (v_{xy}) was assumed as the following.

v_{xy}>0.1m/d $\quad W_h$ =0

0.1m/d > v_{xy} > 0.07m/d $\quad W_h$ =1

0.07m/d > v_{xy} > 0.04m/d $\quad W_h$ =2

v_{xy} < 0.04m/d $\quad W_h$ =3

These threshold values were determined by numerical calculations.

Weightage of vertical groundwater velocity (W_z):

Vertical groundwater flow influences groundwater injection and installing the system in up-flow (discharge) areas is difficult. Hence, weightage in up-flow areas (v_z>0) was assumed as 0 and that in down-flow areas ($v_z \leq 0$) as 1.

Suitability for the ATES system (P) was estimated by using the following expression.

$$P = (W_g + W_h) \times W_z$$

Suitability maps based on above discussion at 20 m, 50 m, and 70 m depths from the surface are shown in **Figure 5.2.3-7**.

Figure 5.2.3-7. Estimated Areas Suitable for ATES System

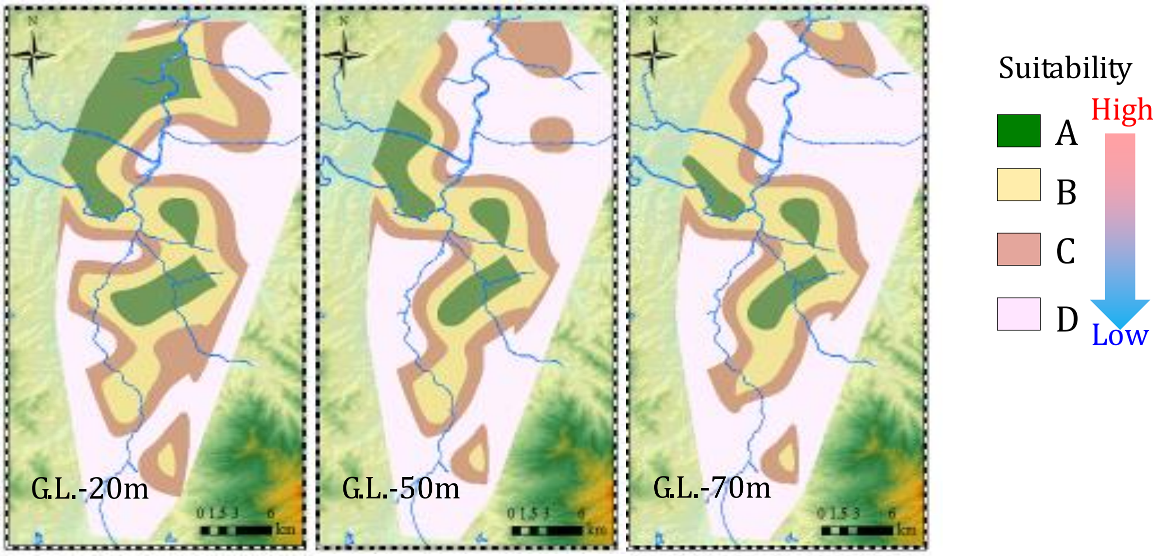

Notes

Source: Yoshioka et al. (2012).

In the legend of **Figure 5.2.3-7**, the suitability rankings A to D represent high to low suitability respectively. The north-western area and central part of the Yamagata Basin were found to have higher suitability. At the north-eastern area, suitability was estimated to be lower. For areas like this, a closed-type GSHP system may be better than an ATES system.

5.2.3.5. Conclusion

In order to evaluate areas suitable for an ATES system in Yamagata Basin, groundwater flow–heat transfer modelling was performed. Computed results were in agreement with both measured groundwater level and subsurface temperature. Some indicative parameters were proposed and applied to the Yamagata Basin, especially horizontal and vertical groundwater flows and geological setting were used. As a result, the area suitable for the system appeared at the central and northwest of the basin. As a future study, results of the field experiment performed in the basin for ATES system will be incorporated in the suitability evaluation.

References

Domenico, P.A. and V.V. Palciauskas (1973), 'Theoretical Analysis of Forced Convective Heat Transfer in Regional Ground-Water Flow', *Geological Survey of America Bulletin*, 84, pp.3803–3814.

Geological Survey of Japan (GSJ) (2004), 'Geothermal Gradient and Heat Flow Data in and around Japan. Geological Survey of Japan', AIST, CD-ROM. (in Japanese with English abstract)

Geological Survey of Japan (GSJ) (2012), 'Water Environment Map No.6 Yamagata Basin. Geological Survey of Japan', AIST, CD-ROM. (in Japanese with English abstract)

Koshigai, M., A. Marui, N. Ito, and T. Yoshizawa (2011), 'Development of Three Dimensional Hydrogeological Model and Estimation of Groundwater Storage in Japanese Islands', *Journal of Japanese Association of Groundwater Hydrology,* 53(4), pp.357–377 (in Japanese with English abstract).

Uchida, Y., Y. Sakura, and T. Arakawa (1993), 'Groundwater Flow Estimated from the Distribution of Subsurface Temperature in Yamagata Basin', *Hydrology*, 23(4), pp.169–179 (in Japanese with English abstract).

Yoshioka, M., Y. Uchida, H. Fujii, and M. Yamaya (2012), 'Groundwater Flow and Heat Transfer Modeling to Estimate the Area Suitable for ATES System,' 3rd International FEFLOW User Conference, p.8.

Lessons learned

- For sustainable use of GSHP systems, system design suitable for the subsurface condition of the location as well as GSHP application purpose is needed.
- Heat exchange rate and preferred drilling depth of a GSHP system varies with local subsurface conditions.
- In this context, a <u>hydrogeological survey is very important for places in sedimentary basins and plains</u>, while only rock properties are important for places with near surface hard rocks.
- To compile suitability maps of GSHP systems for sedimentary regions, groundwater and geological surveys are needed to perform numerical simulations on groundwater flow and local heat exchange rate.
- The design of a GSHP system can be improved by utilising the suitability map, such that high system performance and cost reduction may be achieved.
- A suitability map can be made in the following order of procedures:

1. Groundwater and geological survey
2. Regional groundwater flow simulation
3. Heat exchange simulation of the site
4. Making suitability map
    - Weighted overlay method may be used for making suitability map.
    - For closed-loop system, groundwater velocity, sand-gravel ratio, and water table are used. For open-loop system, horizontal and vertical groundwater flow rate and permeability of geological layers are used.
    - Space heating suitability map needs subsurface temperature data additionally.

5.3. South Korea: Importance of Monitoring and its Data Analysis

5.3.1. Case study 1: Sejong Metropolitan City

Among the active installations of GSHP according to the Renewable Mandatory Act for Public Buildings, there is a notable case in the new central government office building complex in Sejong Metropolitan City. The government building complex is divided into three zones and the total building area reaches 607,555 m^2. Total installed capacity of GSHP exceeds 20 MW_t and covers more than 38 percent of heating and cooling load of the buildings. 70 percent of geothermal energy extraction is from borehole heat exchangers (BHEs) through 1,190 boreholes of 200 m deep and total length of holes reached 238 km. 30 percent of heat exchangers are using ground water wells of around 400 m deep. Zone 1 of the building complex started operation in 2012, Zone 2 in 2013, and Zone 3 was completed in 2014. GSHP for other public buildings including City Hall and the Educational District Buildings in Sejong City are continuously being installed.

Figure 5.3-1. Bird's-eye View of Zones 1 and 2 of the Government Building Complex, Sejong Metropolitan City

Source: www.chungsa.go.kr

Figure 5.3-2. Ground Source Heat Pumps for the Government Building Complex, Sejong Metropolitan City

Note: From top, drilling of borehole for BHE, trench line of heat exchanger pipes into building, and heat pumps in the basement floor of building.
Source: Photo by TurboEnergy Co., Ltd.

The GSHP system in Sejong City is readily equipped with automated monitoring systems and the monitored data are automatically collected at each site. But there is no systematic regulation or organisation for checking and analysing the monitoring data. It is very important not only to monitor the geothermal system, but to analyse the data. Regulations or organisations are needed for making advice on the sustainable use of GSHP systems based on the analysis of results.

5.3.2. Case Study 2: Long-term temperature monitoring in Earthquake Research Center, KIGAM

A long-term monitoring case of ground temperature variation according to GSHP operation can be found at the Earthquake Research Center (ERC) building in South Korea's Institute of Geoscience and Mineral Resources (KIGAM). The building is three storeys high with an area of 700–900 m^2 each, 2,435.4 m^2 in total, and was constructed in 2005. The heating and cooling load is 400 kW. 28 boreholes with a diameter of 165 mm, a depth of 200 m, and 7 m apart were drilled to be installed with double U-tube type borehole heat exchangers (BHE). After installing the BHEs, the top of the BHE were covered with green grasses.

Figure 5.3-3 Earthquake Research Center in KIGAM

Note: During the installation of borehole heat exchangers (BHEs) (left) and after covering BHEs with green grasses (right).
Source: Photo by Tae Jong Lee.

Figure 5.3-4. Layout of Borehole Heat Exchangers and the Monitoring System for the Earthquake Research Center Building at KIGAM

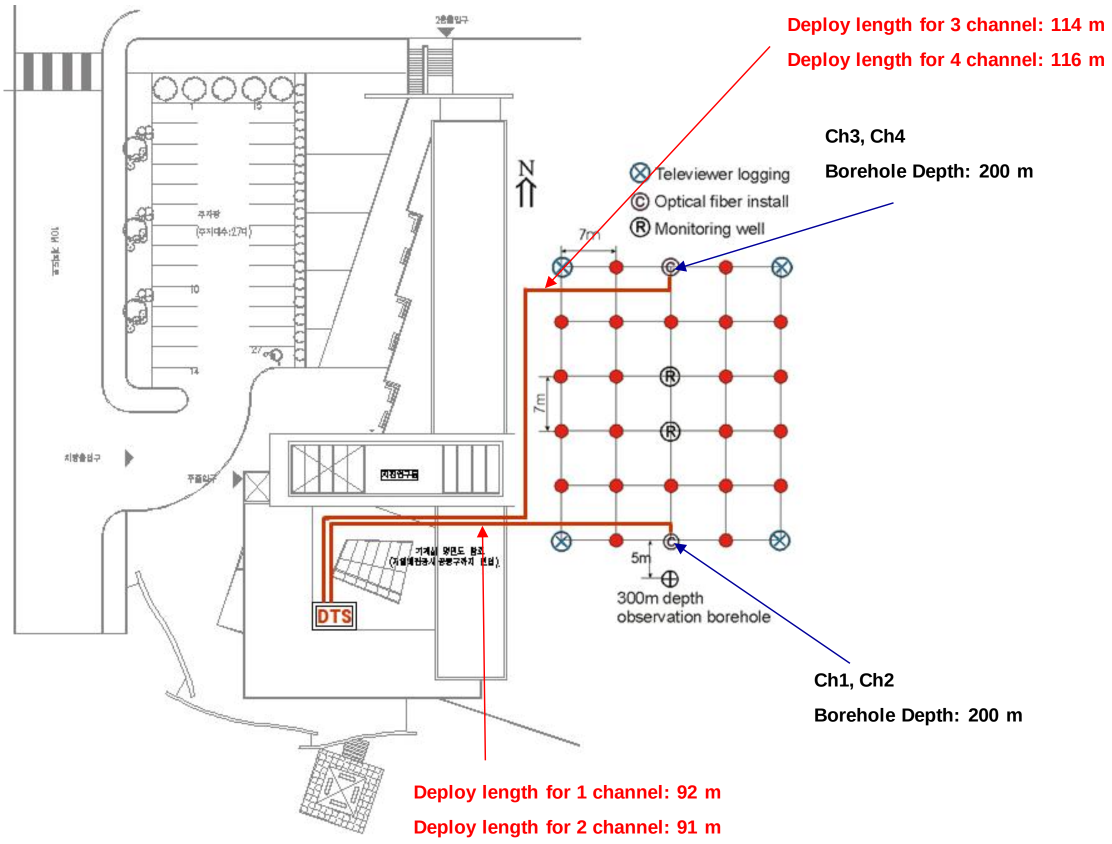

Source: Lee et al. (2010).

The monitoring of the inlet/outlet flow rate and temperature of the BHEs had been performed for about three and half years after the installation. Among 28 BHEs, in addition, fibre optic cables were attached to the outside of U-tubes of two BHEs to monitor the temperature variation with depth. The subsurface temperature beneath the borehole field was getting higher with the GSHP operations and we can see 0.5–1°C of temperature increase per year at 100 m depth (**Figure 5.3-5**). The increase of subsurface temperature was caused by unbalanced seasonal variation of load (actually cooling load is bigger than heating in the building), which may lead to performance degradation as GSHP operation continues year after year. This result is a good example showing that accurate monitoring of the subsurface is important for sustainable use of geothermal energy in heating and cooling applications.

Figure 5.3-5. Comparison of Temperature Variations at 100 Metre Depth Between the Winter Seasons of 2006–2007 and 2008–2009

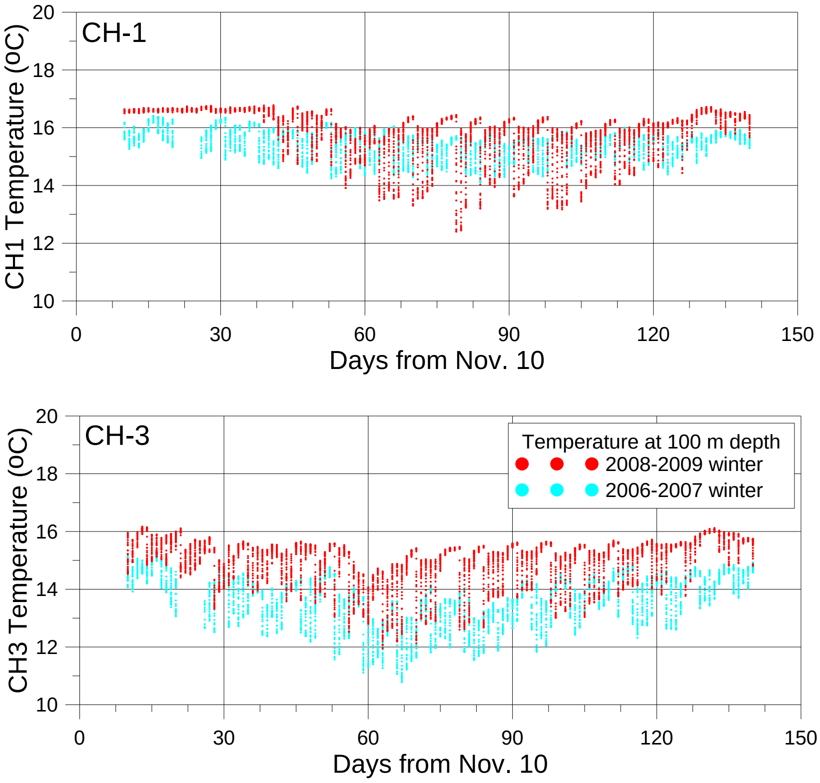

Note: CH-1 and CH-3 denotes the borehole heat exchangers (BHEs) at different locations.
Source: Lee et al. (2010).

In South Korea, by law, all GSHP systems are subject to be monitored in terms of inlet and outlet temperature and flow rates during operation. All these data are collected by the authorised ministry. However, no analysis has been made for these data so that the actual coefficient of performance (COP) has not been calculated, although the COP is the key to understand the effectiveness of GSHP in terms of saving energy, heat extraction, and sustainability.

Lessons learned

- For long-term sustainability, monitoring of the system is important. The monitoring is mandated by law in case of South Korea, but the problem is that the monitoring data has not been properly analysed in many cases.
- Ideally, the subsurface temperature down to the depth of subsurface heat exchanger will be monitored.
- The flow rate and temperature of the primary and secondary fluids and electricity consumption of the heat pump and circulation pump should be monitored to calculate actual COP and long-term performance including extracted heat, amongst others.

Reference

Lee, T. J., Shim, B. O., and Song, Y., 2010, Monitoring of subsurface temperature variation as geothermal utilization, *Journal of Korea Society of Geothermal Energy Engineers*, V. 6, pp. 29–36 (in Korean with English abstract).

5.4. Thailand: Comparison of Groundwater and Atmospheric Temperatures in the Chao-Phraya Plain

Groundwater temperature measurements were widely conducted in the Chao-Phraya Plain in a number of observation wells settled by the Department of Groundwater Resources (DGR), Thailand from 2003 to 2005 (Yasukawa, et al., 2009).

Topographically, the Chao-Phraya plain consists of the upper plain (north of Nakhon Sawan) and the lower plain (south of Nakhon Sawan) with a border around N15°40’, which is also identified by separate shallow groundwater flows (Uchida, et al., 2009). Locations of observation wells are shown in **Figure5.4-1**.

Figure 5.4-1. Contour Map of Maximum Temperature at Depths of 20–50 m (°C)

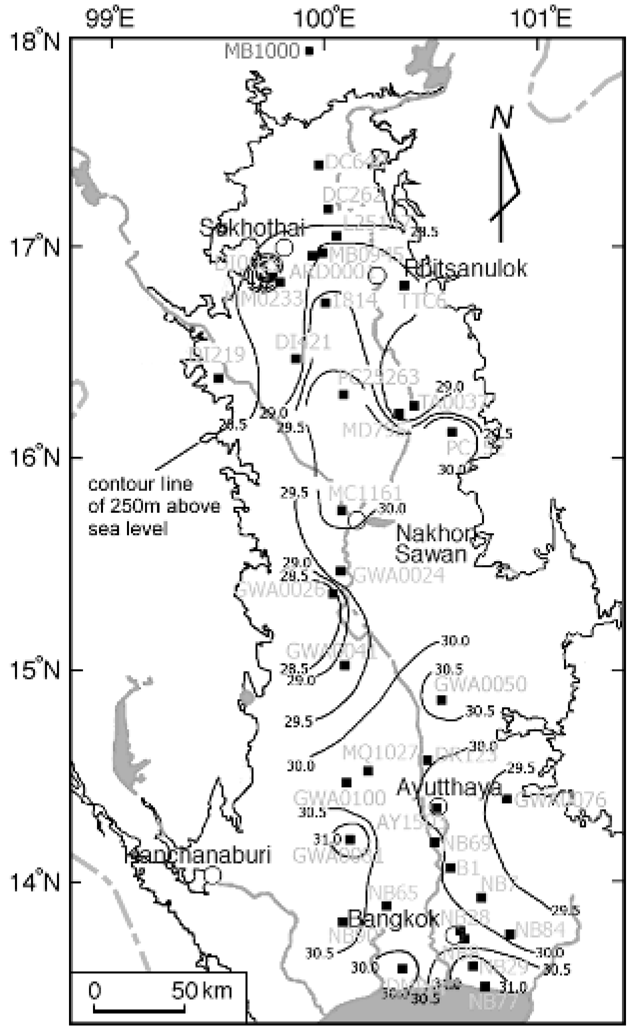

Note: Location of observation wells are shown by black square.
Source: Yasukawa, et al. (2006a).

Figure 5.4-2. Temperature Profiles of Wells in Certain Areas in Thailand

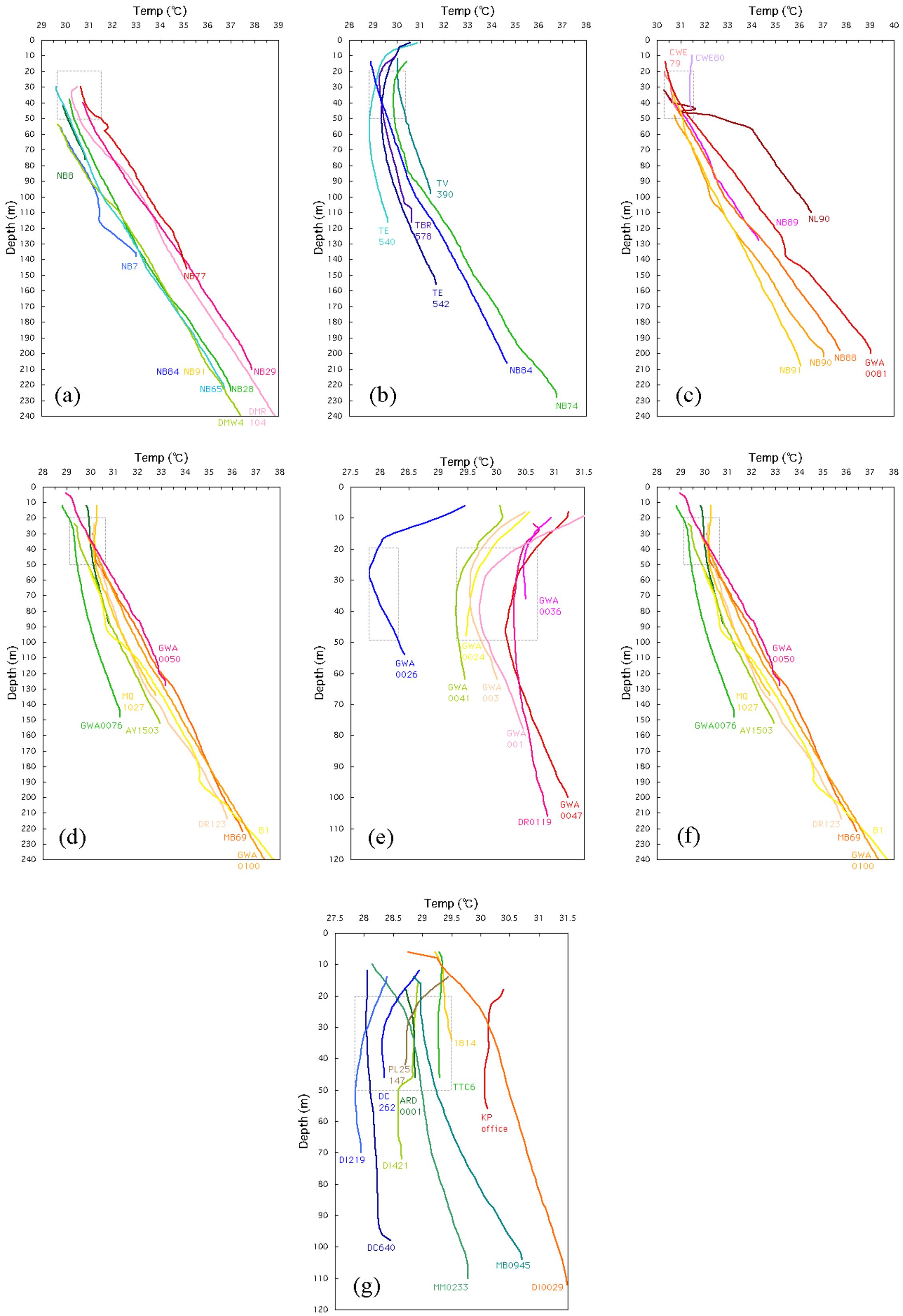

Notes: (a) Bangkok, (b) Bangkok East, (c) Kanchanaburi, (d) Ayutthaya, (e) Nakhon Sawan south, (f) Nakhon Sawan north, and (g) Phitsanulok-Sukhothai areas.
Temperature ranges at a depth from 20m to 50 m are indicated by grey rectangles.
Source: Yasukawa, et al. (2006b).

Figure 5.4-2 shows the observed temperature profiles in these wells. For GSHP systems for cooling, the proper depth of heat exchange wells may be around 50 m or less, since the subsurface temperature increases with depth and deep wells are not appropriate as a ‘cool’ heat source. Therefore the temperature range at depths between 20 to 50 m in each area is indicated in **Figure 5.4-2**. The temperature at depths shallower than 20 m is ignored because it may be affected by daily and seasonal changes so that the observed value may not represent the statistical mean. In the whole Chao Phraya plain, temperature at depths between 20 to 50 m ranges from 27.8^{o}C (GWA0026, DI219) to 31.5^{o}C (NB77, GWA0081).

Figure 5.4-1 shows a contour map of maximum temperature in these depths. Generally the wells in the upper basin have a lower subsurface temperature than those in the lower basin. However, GWA0041 (**Figure 5.4-2(c)**) and GWA0076 (**Figure 5.4-2(b)**) in the lower basin have rather low temperatures with profiles characteristic to the recharge zone. These wells are considered to be located in local recharge zones of the lower basin for shallow groundwater flow. Shallow local flows may exist in upper and lower basins, respectively.

Figure 5.4-3. Comparison of Atmospheric and Subsurface Temperature at Each Region

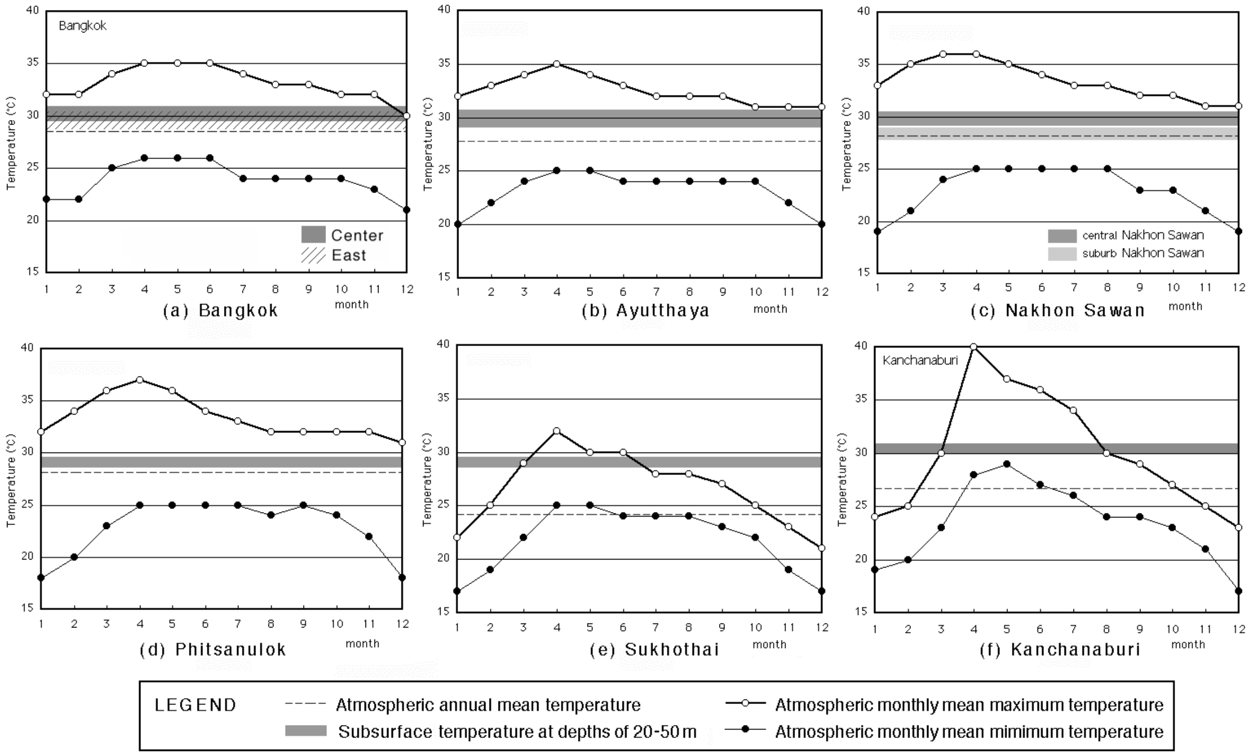

Source: Yasukawa, et al. (2006a).

Figure 5.4-3 compares atmospheric and subsurface temperatures in depths between 20 to 50 m at (a) Bangkok, (b) Ayutthaya, (c) Nakhon Sawan, (d) Phitsanulok, (e) Sukhothai, and (f) Kanchanaburi regions. The subsurface temperature data from wells NB29 and NB77, both located near the sea, with extremely high temperature, are eliminated for **Figure 5.4-3(a)**. Subsurface temperatures shown in **Figure 5.4-3(d)** and **Figure 5.4-3(e)** are identical because they are based on data from the same region, while the atmospheric temperatures are different.

At Pitsanulok and Nakhon Sawan, the subsurface temperature is lower than the monthly mean maximum atmospheric temperature (mmmax) through a year. Its difference is higher than 5 Kelvin (K) over four months. Also at Kanchanaburi, the subsurface temperature is lower for 5K or more over four months with a largest difference of 10K in April. A GSHP system may be used in these areas for space cooling especially in daytime. In Bangkok and Ayutthaya, the subsurface temperature is lower than mmmax for almost through a year, but the difference is 5K or less, so performance of a GSHP system may be lower in these regions. In Sukhothai, where the subsurface temperature is higher than mmmax for most of the year, underground may not be used as a ‘cold heat-source’.

Lessons learned

For GSHP application in tropical regions where only space cooling is needed, the underground temperature should be measured first to ensure the applicability of the GSHP system.

If the underground is cooler than atmosphere at least in daytime, GSHP may be effective.

Thus as results of the comparison of underground and atmospheric temperatures, applicability of a GSHP system is shown for many cities in Thailand.

References

Uchida, Y., K. Yasukawa, N. Tenma, Y. Taguchi, J. Suwanlert, and S. Buapeng (2009), ‘Subsurface Thermal Regime in the Chao-Phraya Plain’, Thailand. *Bulletin of Geological Survey Japan*, 60, pp.469–489.

Yasukawa, K., Y. Uchida, Y. Taguchi, N. Tenma, H. Muraoka, S. Buapeng, and T.H. Nguyen (2006a), ‘Possible Utilization of Ground-coupled Heat-pump System in Tropical Countries’, in *Proceedings of the 7th Asian Geothermal Symposium, 25–26 July, 2006, Qindao, China*, pp.159–164.

Yasukawa, K., Y. Uchida, Y. Taguchi, and S. Buapeng (2006b), ‘Possibility of GSHP Application in Thailand’, EIT-JAPAN-AIT Seminar on Geo-Risk Engineering-Monitoring and Geo-Exploration, 27 September 2006, Bangkok, Thailand.

Yasukawa, K., Y. Uchida, N. Tenma, Y. Taguchi. H. Muraoka, T. Ishii, J. Suwanlert, S. Buapeng, and T.H. Nguyen (2009), ‘Groundwater Temperature Survey for GSHP Application in Tropical Asia’, *Bull. Geol. Surv. Japan*, 60, pp.469–467.

5.5. Viet Nam: Comparison of Groundwater and Atmospheric Temperature in the South Plain and the Red River Plain

5.5.1. Initial possibility evaluation to install GSHP in Southern Plain of Viet Nam

5.5.1.1. Introduction of the groundwater observation system in Viet Nam

The groundwater observation activities in Viet Nam have started in three main economic areas, the Southern Plain, the Northern Plain, and the Central Highlands, since 1990s with 259 observation places consisting of 515 observation wells (**Figure 5.5.1-1**). Recently, the system of groundwater observation places has been extended in the North Central Coastal areas and South Central Coastal areas with a total of 707 groundwater observation wells. Besides, some provinces have developed individual groundwater observation wells, which are not indicated in this report.

Figure 5.5.1-1. Three National Groundwater Observation Networks Developed Since 1995

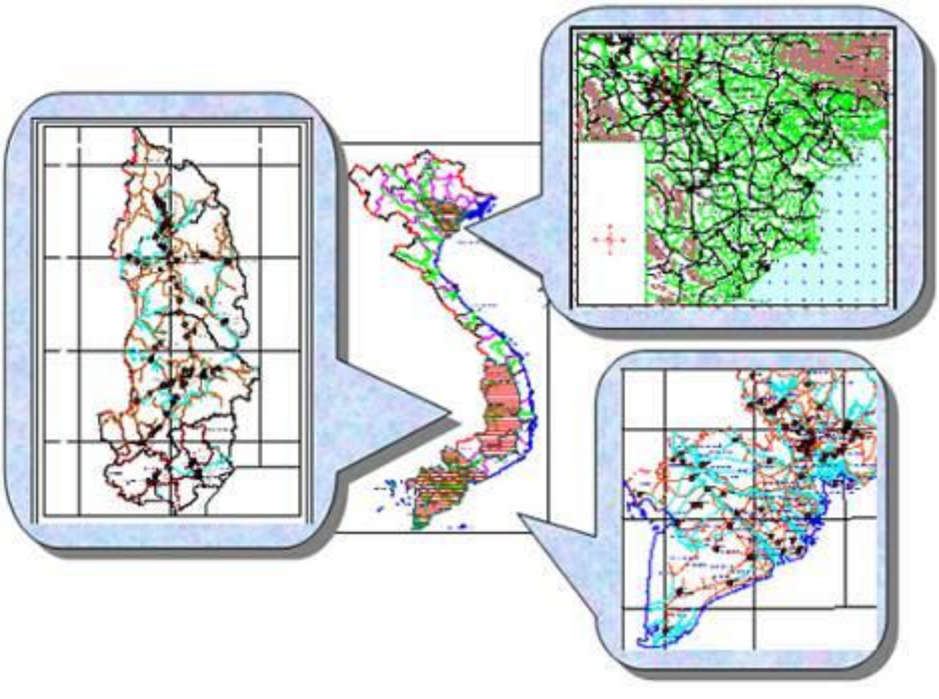

Source: NDWRPI (2009).

Each groundwater observation network consists of many observation places. Some observation places have only one observation well but others have a cluster of wells that are quite close to each other (a few to tens metres). Each observation well is used for monitoring groundwater behaviour of a certain aquifer. The periodically observed parameters are water level, flow rate, flow velocity, temperatures, chemical composition, gas contents, and microbes.

Based on MONRE (2013) on stipulation of the groundwater observation technique, groundwater temperatures are measured manually or automatically in these wells. For a manually observed well that is not affected by tide, the temperature is measured soon after measuring the water level. For a manually observed well that is affected by tide, the temperature is measured once a day at 1300 hours. For an automatically observed well, the temperature is measured five times a month at inspection and maintenance time of the equipment. The measuring probe is placed at any position in the filter tube that is cased in the aquifer. Practically, most of the temperatures are measured when the measuring probe is submerged in the groundwater of the aquifer. The accuracy of measurement is 0.5K. From 2010 to now, most of the observation temperatures are automatically measured.

5.5.1.2. Introduction to the groundwater observation network in the Southern Plain

The Southern Plain, with an area of 57.000 km^2, is formed by the Me Kong and Dong Nai river deltas in the South of Viet Nam. The basement rock is friability Quaternary and Neogene with the thickness from 500-600 m lying on the Mesozoic–Paleozoic consolidated formations. The observation network is spread out 66 places with 189 wells.

The terrain of the Southern Plain is relatively flat and has some low hills in the north-western part that makes the boundary with Cambodian territory. The north-eastern part is the beginning of the central highlands, so the elevation is also increasing gradually. The coastal lines are surrounded on the east and the west sides. There are only some observation wells at an elevation of 70 m located in the north-east (Dong Nai and Binh Phuoc provinces). The rest of the observation wells are located mainly at the elevation of less than 20 m.

With the aim to evaluate the possibility of GSHP for cooling, a set of groundwater temperature observation data is used to analyse and interpret so that the initial evaluation on the capability to install the GSHP is introduced for the Southern Plain.

Because there are no temperature measurement data in detail for each observation well (for example, temperatures measured in 2 m interval), the statistic data of observation wells from NDWRPI (2011) are used. As many of those observation places have plural observation wells with different screen depth, places with at least two observation wells are selected for this study. Since the wells at one place are very close each other, all the temperature data from one place are considered as temperature data from deferent depths of one well.

From 66 observation places with 189 wells, 14 places with 50 wells have been selected in the areas of Ho Chi Minh, Tay Ninh, An Giang, Ca Mau, and Tra Vinh. The wellhead elevation of these wells varies from 1 m to 20 m (**Table 5.5.1-1**). The well locations are shown in **Figure 5.5.1-2**.

Among 50 observation wells, 23 wells are affected by tide. The wells in Tay Ninh province are not affected by tide and located at the highest elevation (from 4.8 to 19.8m) (**Table 5.5.1-1**), while the most of wells in Ca Mau and Tra Vinh provinces are affected by tide and located at the lowest elevation (from 1.15 to 2.54 m). The distances between the wells in one province varied from 1 km to 50 km.

Table 5.5.1-1. Monthly Mean Temperatures of Groundwater at Deferent Aquifers in the Observation Wells in South Plain, Viet Nam

No.	Area	Observation place	Well	Aqu.	Depth (m) from	Depth (m) to	Tid.	Location x	Location y	Location z (m)	Month 1	2	3	4	5	6	7	8	9	10	11	12
1	HCM City	Q808	Q808010	qh	20	29	y	1192962	665306	1.23	28.5	28.5	28.5	28.7	28.6	28.6	28	27.4	28	27.9	27.5	27
2			Q808020	qp_3	29	77	y	1192970	665306	1.36	28.6	28.4	28.5	28.8	28.6	28.6	28	27.4	28	27.9	27.5	27
3			Q808030 M1	qp_{2-3}	86.9	133.5	y	1192981	665317	1.24	28.5	28.4	28.5	28.5	28.6	28.6	28	27.4	28	27.9	27.5	27
4			Q808040	n_2^2	173.5	207.5	y	1192979	665312	1.4	28.5	28.6	28.3	28.5	28.6	28.6	28	27.4	28	28	27.5	27
5			Q808050 M1	n_1^3	257.5	313	y	1192974	665315	1.31	28.5	28.4	28.5	28.5	28.6	28.6	28	27.4	28	27.9	27.5	27
6		Q804	Q804020	qp_3	0	28	n	1215192	664143	10.2	29.5	29	29	29	29	30	30	30	30	30	30	30
7			Q80404T	n_2^2	64.8	119.6	n	1215189	664144	10.3	30	30	30	30	30.3	30.5	30.5	30.5	30.5	30.5	30.5	30.3
8			Q80404Z M1	n_2^1	124.6	179.5	n	1215188	664143	10.3	30	30	30	30	30.3	30.5	30.5	30.5	30.5	30.5	30.5	30.3
9		Q011	Q011020	qp_3	0	32	n	1201413	676370	7.91	28	28	28.3	29	29.3	27.6	27.5	27.5	27.5	26.8	27.3	25.9
10			Q011340	qp_{2-3}	48	70	n	1201404	676357	8.1	28	28	28	29	29.3	27.6	27.6	27.5	27.5	26.8	26.3	25.9
11			Q011040	n_2^2	130	174	n	1201398	676357	8.05	28	28	28.3	29	29	27.6	27.4	27.5	27.5	26.8	26.3	25.9
12		Q002	Q00202A	qp_{2-3}	25	49	y	1214361	679458	1.94	27.5	27.5	27.5	27.5	27.5	27.5	27	27	27	27	27	27
13			Q00204A	qp_1	50.9	75	y	1214361	679462	2.15	27.5	27.5	27.5	27.5	27.5	27.5	27.5	27.5	27	27	27	27
14	Tay Ninh	Q221	Q221020	qp_3	0	23	n	1250383	618306	4.8	28	29	29	29	29	29	29	29	28	28	28	28.2
15			Q22104T	qp_1	37	77	n	1250381	618299	4.63	29	29	29	29	29	29	29	29	29	29	29	29
16			Q22104Z	n_2^2	81.4	141.5	n	1250381	618294	4.54	29	29	29	29	29	29	29	29	29	29	29	29
17		Q023	Q023020 M1	qp_3	8.5	15	n	1219729	648145	5.39	29	29	29	29	29	29	29	29	29	29	29	29
18			Q02304T M1	qp_1	41.5	54.5	n	1219729	648145	5.41	29	29	29	29	29	29	29	29	29.1	29	29	29
19			Q02304Z M1	n_2^1	93.2	114.7	n	1219729	648145	5.42	30	30	29.9	30	30	30	30	30	30	30	30	30
20			Q023050 M1	n_1^3	114.7	141.5	n	1219730	648146	5.41	30	30	29.9	30	30	30	30	30	30	30	30	30
21		Q220	Q22002T	qp_3	0	4.5	n	1282515	607651	19.9	29	29	29	29	29	29	29	29	29	29	29	29
22			Q22002Z	qp_{2-3}	4.5	32	n	1282520	607650	19.9	30	30	30	30	30	30	30	30	30	30	30	30
23			Q220040 M1	qp_1	38.8	77	n	1282535	607647	19.8	30	30.6	31	31	31	31	31	31	31	31	31	31
24			Q220050 M1	n_2^1	118	179.5	n	1282538	607647	19.8	30	30.6	31	31	31	31	31	31	31	31	31	31

25	An Giang	Q203	Q20302TM1	qh	15	38	n	1186763	518233	5.06	30	30	29	30	30	30	30	30	30	30	30	30
26			Q20302ZM1	qp_3	45	75	n	1186763	518233	5.06	30	30	29	30	30	30	30	30	30	30	30	30
27			Q203040M1	qp_{2-3}	77	93	n	1186763	518233	5.07	29	29	29	29	29	29	29	29	29	29	29	29
28		Q204	Q20400S	nm	0	0	n	1156229	531843	3.44	29	29	29	29	29	29	29	29	29	29	29	29
29			Q204010	qh	0	32.8	n	1156175	532012	3.4	29	29	29	29	29	29	29	29	29	29	29	29
30			Q20402T	qp_3	42	49	y	1156180	532016	3.4	29	29	29	29	29	29	29	29	29	29	29	29
31			Q20402Z	qp_{2-3}	76.2	130	y	1156182	532017	3.44	29	29	29	29	29	29	29	29	29	29	29	29
32			Q204040	n_2^2	162	182	y	1156184	532019	3.47	29	29	29	29	29	29	29	29	29	29	29	29
33	Ca Mau	Q177	Q17701T	qh	0	29.5	n	1016287	516372	1.16	27.1	27.3	27.5	27.5	27.3	27.2	27.7	28	28	27.4	27.9	28
34			Q17701ZM1	qp_3	43.5	58.1	n	1016292	516374	1.15	28	27.6	27.5	28	28.1	27.2	27.9	28.1	28	27.7	28	28.4
35			Q177020M1	qp_{2-3}	82	96.2	n	1016290	516372	1.21	29	29	29	29	29	28	29	29	29	28.7	29	29
36			Q17704TM1	n_2^2	165.5	236.6	y	1016287	516375	1.16	29	29	29	29	29	29	29	29	29	28.9	29	29
37			Q17704ZM1	n_2^1	260	273	y	1016291	516377	1.17	29	29	29	29	29	29	29	29	29	28.9	29	29
38		Q188	Q188020	qp_{2-3}	41.5	122	y	1014731	516404	1.73	29	29	29	29	29	29	29	29	29	28.8	29	29
39			Q188030	qp_1	122	185	n	1014730	516405	1.75	28.5	28.1	28.1	28.6	28.2	28.3	28.2	28.2	28.1	28.3	28.1	28.4
40		Q199	Q199010	qh	0	40	y	968465	499584	1.14	28	28	28	28	28	28	28	28	28	28	28	28
41			Q19904T	n_2^2	224.9	250.5	y	968461	499586	1.11	31	31	31	31	31	31	31	31	31	31	31	31
42			Q19904ZM1	n_2^1	294.5	322.4	y	968458	499551	1.03	31	31	31	31	31	31	31	31	31	31	31	31
43	Tra Vinh	Q217	Q217010	qh	0	26	n	1065368	663815	2.54	27.6	27.9	28	28	28	27.7	27.8	27.7	27.7	27.7	27.3	27.7
44			Q217020	qp_{2-3}	100	152	y	1065369	663817	2.39	27.5	27.5	28	28	28	28	28	27	27	27.5	27.5	27
45			Q217030	n_2^2	242.5	313	y	1065371	663821	2.45	27.5	27.5	28	28	28	28	28	27	28	28	28	28
46			Q217040	n_2^1	322	381	y	1065372	663824	2.49	27.5	27.5	28	28	28	28	29	29	27.5	29	29	29
47		Q404	Q404020	qp_3	27	128	y	1076961	638467	1.58	28	28	28	29	29	28	27	27.3	28	27.7	28.2	27.7
48			Q40403T	qp_{2-3}	128	174	y	1076985	638470	1.58	29	29	29	29	29	28.5	28	27.8	28.5	28.2	28.7	28
49			Q40403Z	n_2^2	237	285	y	1076958	638470	1.58	29	29	29	29	29	29	28.5	28.3	29	28.7	29.2	28.5
50			Q40404TM1	n_2^1	317	377	y	1076960	638473	1.74	30	30	30	30	30	29.5	27	28.8	29.5	29.2	29.7	29

Aqu. = aquifer layer; Tid. = aquifer is affected by tidal: y = yes or n = no; z = elevation of ground surface at observation well.
Source: NDWRPI (2011).

Figure 5.5.1-2. Groundwater Observation Places in Southern Plain

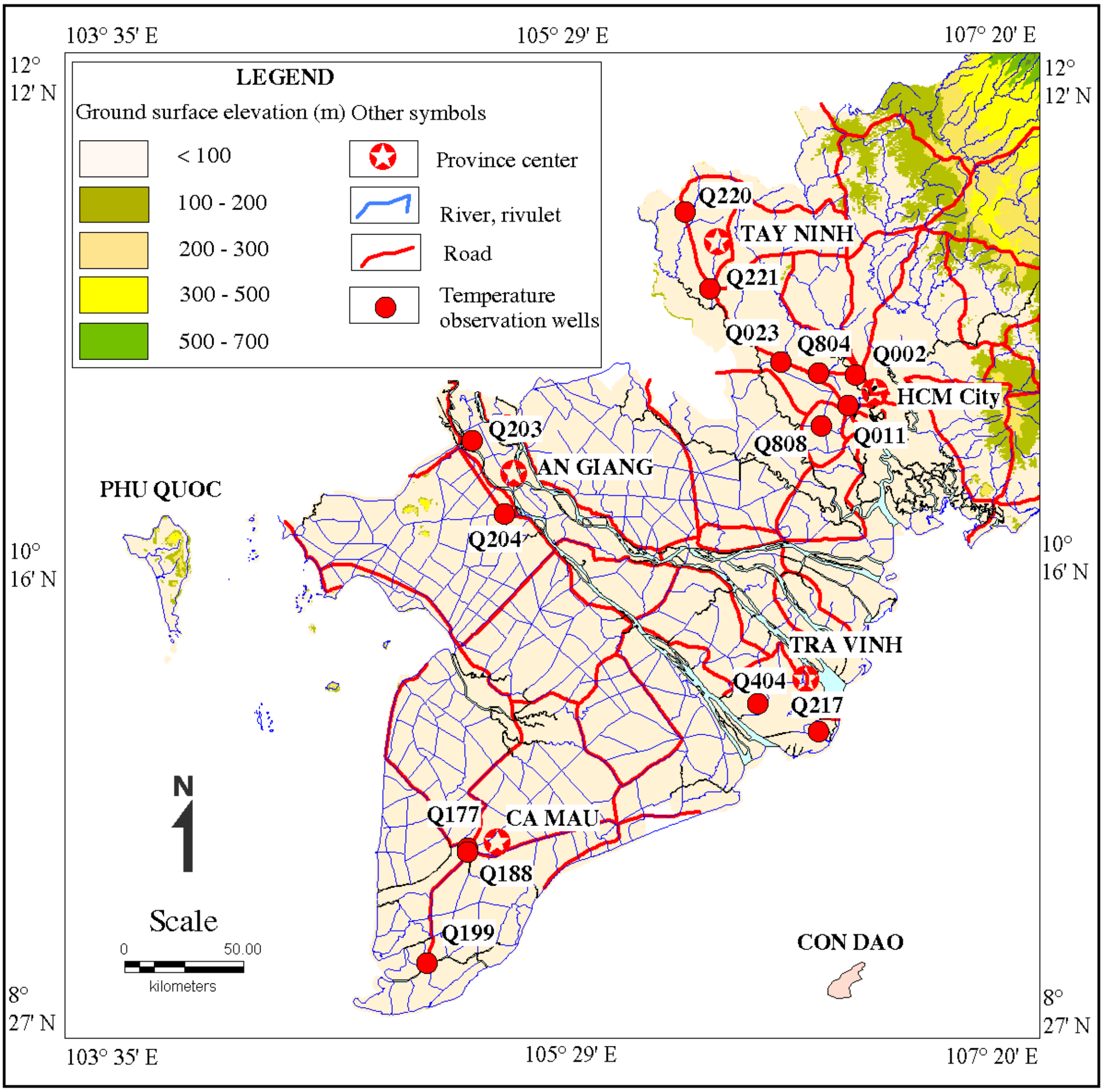

Source: NDWRPI (2011).

5.5.1.3. Climate characteristics in Southern Plain

The Southern Plain is situated in the typical monsoon tropical and subequatorial area with abundant humid heat-base, plentiful sunlight, long radiation time, and high temperature. The day and night temperature change among months of a year is low and moderate. Annual average humidity ranges from 80–82 percent. There are two seasons in a year: dry and rainy. The rainy season is from May to November and the dry season is from December to April. The highest and lowest temperatures of every month in Ho Chi Minh and Ca Mau areas are presented in **Tables 5.5.1-2** and **5.5.1-3**.

Table 5.5.1-2. Groundwater and Atmospheric Temperatures in Ho Chi Minh

Month / Temperature (°C)	Jan	Feb	Mar	Apr	May	Jun	Jul	Aug	Sep	Oct	Nov	Dec
Monthly mean maximum of air	32	32	33	34	35	34	33	32	33	33	32	33
Monthly mean of ground water	28	28	28	28	28	28	28	28	28	28	28	28
Monthly mean minimum of air	21	22	23	25	25	24	24	24	24	23	23	22

Source: Compiled by authors based on NCHMF (2015) and NDWRPI (2011).

Table 5.5.1-3. Groundwater and Atmospheric Temperatures in Ca Mau

Month / Temperature (°C)	Jan	Feb	Mar	Apr	May	Jun	Jul	Aug	Sep	Oct	Nov	Dec
Monthly mean maximum of air	25	26	33	35	35	33	33	33	33	33	32	30
Monthly mean of ground water	29	29	29	29	29	29	29	29	29	29	29	29
Monthly mean minimum of air	22	22	23	25	25	24	24	24	24	23	22	20

Source: Compiled by authors based on NCHMF (2015) and NDWRPI (2011).

5.5.1.4. Comparison of atmospheric and groundwater temperatures

Since most of the aquifers lie at depths of dozens to hundreds of metres, the temperatures are relatively stable through a year. The average values of groundwater temperature measured from January to December were used to compare with atmospheric temperature. The measuring points are few metres deeper than the water level in the wells (hydraulic head of the aquifer) because the measuring probe should be submerged into the water. Since temperatures at deeper levels are not available, these measured temperatures at slightly deeper than the water level of each well were used. The measured temperatures are about 27 to 30°C in Ho Chi Minh and 27 to 31°C in Ca Mau areas.

The minimum and maximum temperatures in each month and the range of subsurface temperatures in Ho Chi Minh and Ca Mau areas are presented in **Tables 5.5.1-2** and **5.5.1-3**. From these tables, the diagrams of subsurface and atmospheric temperature comparisons are made as shown in **Figs. 5.5.1-3** and **5.5.1-4.** These figures indicates that GSHP may be used for cooling in Ho Chi Minh area throughout the year while GSHP may be used for cooling in Ca Mau from March to November.

Figure 5.5.1-3. Comparison of Atmospheric and Groundwater Temperatures in Ho Chi Minh

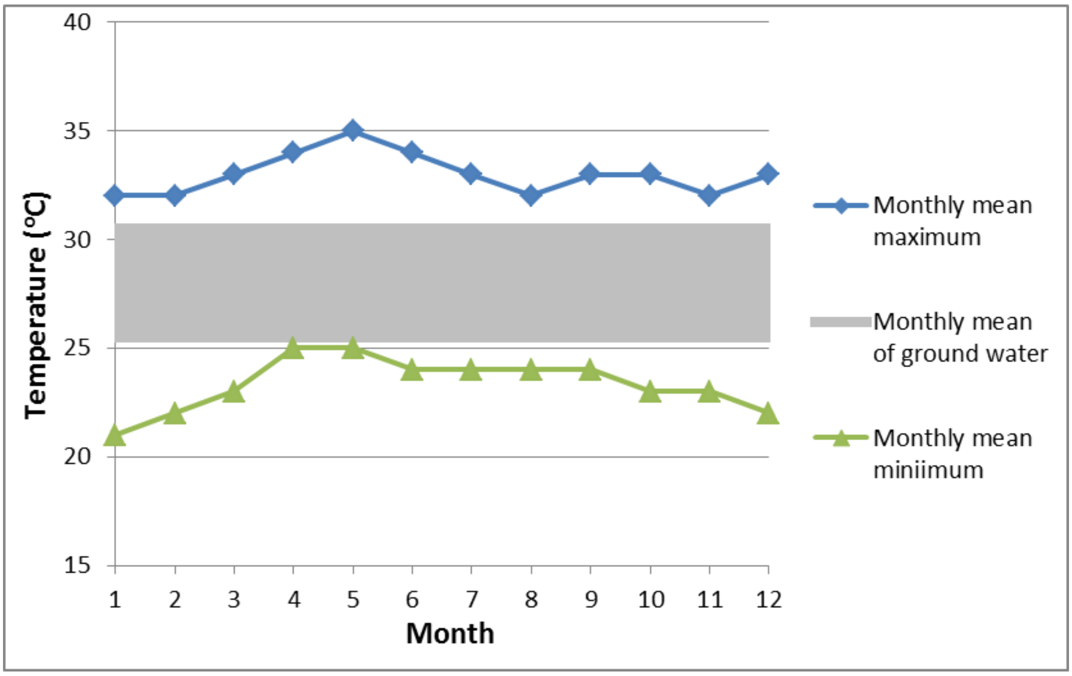

Source: Edited by authors based on NCHMF (2015) and NDWRPI (2011).

Figure 5.5.1-4. Comparison of Atmospheric and Groundwater Temperatures in Ca Mau

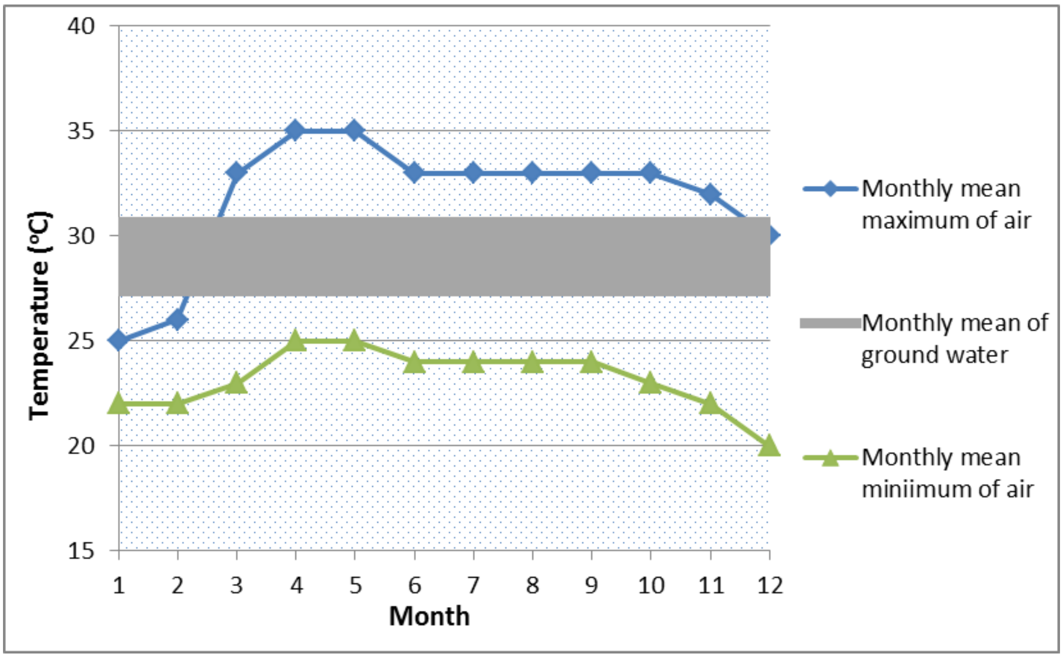

Source: Edited by authors based on NCHMF (2015) and NDWRPI (2011).

Lessons learned and recommendations

- Monthly mean maximum atmospheric temperature in the Southern Plain is hot and sunny almost all year round so the GSHP may be installed for cooling.
- The variances between atmospheric and groundwater temperatures can help to initially predict the capability of installing the GSHP in many areas in the Southern Plain of Viet Nam.
- The observation wells can be used to evaluate the subsurface temperatures so that the possibility of GSHP may be evaluated in Viet Nam.
- To extract the suitable areas for GSHP systems, more detailed investigations including suitability mapping based on hydrogeological data should be conducted. As for areas where the GSHP can be applied, a pilot system installation and operation including subsurface temperature monitoring is recommended before distribution of the systems.

References

Ministry of Natural Resources and Environment. (MONRE) (2013), 'Circular on Stipulation of Groundwater Observation Technique', 19/2013/TT-BTNMT 18 July 2013.

National Division for Water Resources Planning and Investigation (NDWRPI) (2009), 'Introduction to Groundwater Observation Network', National Division for Water Resources Planning and Investigation, Ministry of Natural Resources and Environment of Vietnam.

NCHMF (2015) Website of the National Centre for Hydro-Meteorological Forecasting. Ministry of Natural Resources and Environment, Viet Nam.

NDWRPI (2011), *Year Book 2010. Groundwater Resource in Southern Plain of Vietnam,* National Division for Water Resources Planning and Investigation, Ministry of Natural Resources and Environment.

Yasukawa, K., Y. Uchida, N. Tenma, Y. Taguchi. H. Muraoka, T. Ishii, J. Suwanlert, S. Buapeng, and T. H. Nguyen 2009), 'Groundwater Temperature Survey for Geothermal Heat Pump Application in Tropical Asia', *Bulletin of the Geological Survey of Japan,* 60(9/10), pp.463–466.

5.5.2 Temperature survey at the Red River Plain, Viet Nam

A groundwater temperature survey was conducted in the Red River plain in observation wells operated by the Department of Geology and Minerals of Viet Nam (DGMV) in 2005 and 2006 (Yasukawa, et al., 2009). Although this region is not a tropical area, it is important to know the subsurface temperature distribution around this area in order to compare with the southern part of the country.

The location of observation wells in this area, for which temperature profiles are obtained, are shown in **Figure 5.5.2-1. Figure 5.5.2-2** shows the observed temperature profiles for these wells. The colour of each profile corresponds to that of wells in **Figure 5.5.2-1**.

Figure 5.5.2-1. Locations of Temperature Observation Wells in the Red River Plain

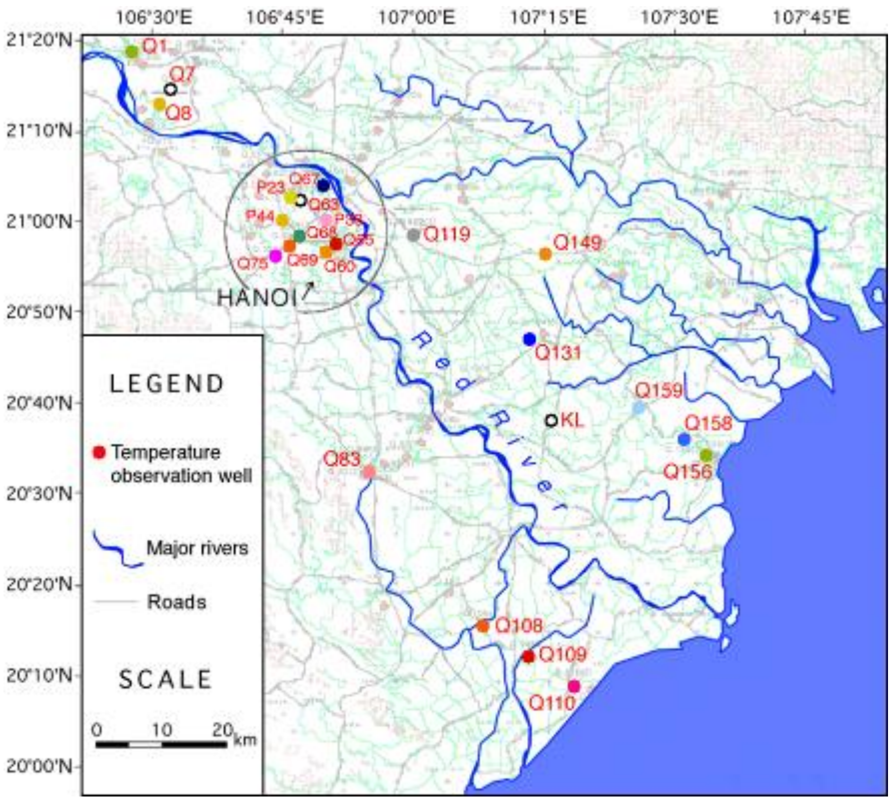

Source: Yasukawa, et al. (2006).

In the south of the Red River, the wells near the sea (Q108, Q109, Q110) show higher a temperature gradient than those at Ha Noi (inner land), indicating the difference of discharge and recharge zones as shown in **Figure 5.5.2-2**. However in the north of the

Red River, the wells near the sea (Q156, Q158, Q159, Q131, etc.) have lower a temperature gradient than those in Ha Noi. It suggests that the groundwater system in the north is different from that along the Red River. Amongst the ones in the north, wells near the sea have a higher temperature gradient.

Figure 5.5.2-2. Temperature Profiles of the Wells around Ha Noi

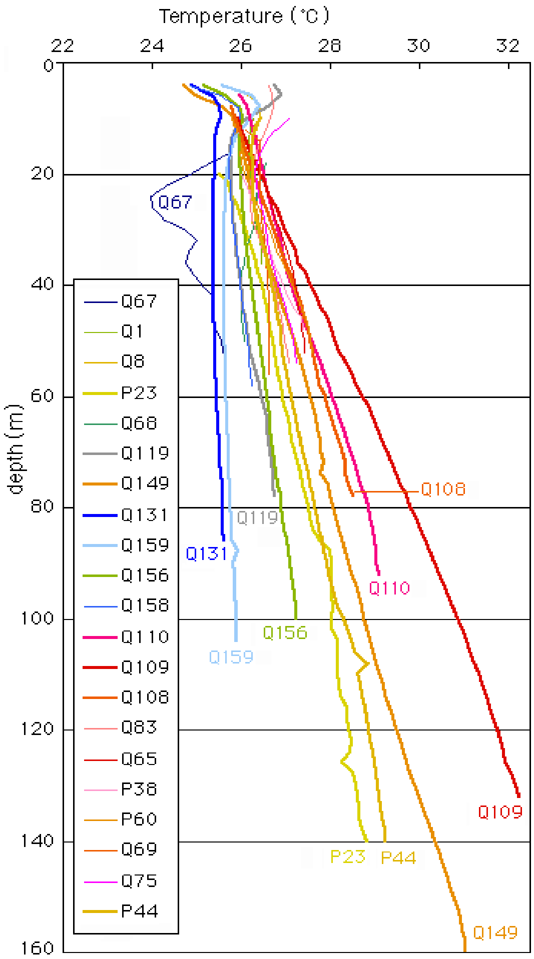

Source: Yasukawa, et al. (2006).

Figure 5.5.2-3 shows monthly change of atmospheric temperature at Ha Noi and groundwater temperature at depths of 20–50m, observed at wells shown in a grey circle in **Figure 5.5.2-1**. In Ha Noi, the subsurface temperature is lower than the monthly mean maximum atmospheric temperature (mmax) from May to October for 5K or more. Therefore, underground may be used as a 'cold heat source' in the summer season. On the other hand, in the winter season, the underground temperature is higher than the atmospheric temperature and it can be used as a hot heat source. Although winter air temperature in Ha Noi is not very low, the humidity is so high that GSHP as a heating system would be useful for drying.

Figure 5.5.2-3. Comparison of Atmospheric and Subsurface Temperature Around Ha Noi

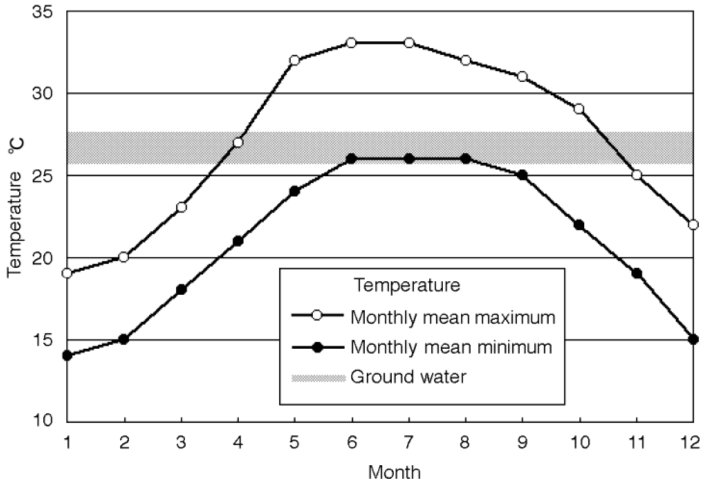

Source: Yasukawa, et al. (2006).

Lessons learned

For GSHP application in tropical regions, the ground temperature should be measured first to ensure the applicability of the GSHP system in terms of temperature advantage.

If the underground temperature is lower than the atmosphere at least in daytime, GSHP may be effective. Thus temperature survey results shows the applicability of a GSHP system in Ha Noi.

References

Yasukawa, K., Y. Uchida, Y. Taguchi, N. Tenma, H. Muraoka, S. Buapeng, and T.H. Nguyen (2006), 'Possible Utilization of Ground-coupled Heat-pump System in Tropical Countries', in *Proceedings of the 7th Asian Geothermal Symposium, 25–26 July 2006, Qindao, China*, pp.159–164.

Yasukawa, K., Y. Uchida, N. Tenma, Y. Taguchi. H. Muraoka, T. Ishii, J. Suwanlert, S. Buapeng, and T.H. Nguyen (2009), 'Groundwater Temperature Survey for GSHP Application in Tropical Asia', *Bulletin of Geological Survey Japan*, 60, pp.469–467.